mathematics

MDPI

Review

Homogeneously Weighted Moving Average Control Charts: Overview, Controversies, and New Directions

Jean-Claude Malela-Majika [1,*], Schalk William Human [1] and Kashinath Chatterjee [2]

[1] Department of Statistics, Faculty of Natural and Agricultural Sciences, University of Pretoria, Hatfield, Pretoria 0028, South Africa
[2] Department of Biostatistics and Data Science, Augusta University, Augusta, GA 30912, USA
* Correspondence: malela.mjc@up.ac.za

Abstract: The homogeneously weighted moving average (HWMA) chart is a recent control chart that has attracted the attention of many researchers in statistical process control (SPC). The HWMA statistic assigns a higher weight to the most recent sample, and the rest is divided equally between the previous samples. This weight structure makes the HWMA chart more sensitive to small shifts in the process parameters when running in zero-state mode. Many scholars have reported its superiority over the existing charts when the process runs in zero-state mode. However, several authors have criticized the HWMA chart by pointing out its poor performance in steady-state mode due to its weighting structure, which does not reportedly comply with the SPC standards. This paper reviews and discusses all research works on HWMA-related charts (i.e., 55 publications) and provides future research ideas and new directions.

Keywords: homogeneously weighted moving average; double HWMA; conditional expected delay; HWMA; memory-type chart; Monte Carlo simulation; steady-state mode; triple HWMA; weight structure; zero-state mode

MSC: 62P30; 62F10; 62G05

Citation: Malela-Majika, J.-C.; Human, S.W.; Chatterjee, K. Homogeneously Weighted Moving Average Control Charts: Overview, Controversies, and New Directions. *Mathematics* **2024**, *12*, 637. https://doi.org/10.3390/math12050637

Academic Editor: Takeshi Emura

Received: 26 December 2023
Revised: 15 February 2024
Accepted: 16 February 2024
Published: 21 February 2024

1. Introduction

Control charts are simple graphs used to identify which type of variation exists within a process to determine whether the process is stable or not. The chart shows the value of the quality characteristic versus the time. Thus, it consists of a charting statistic on the vertical axis, the time on the horizontal axis, a centreline representing the charting statistic's mean, and two horizontal lines, called the lower control limit (LCL) and the upper control limit (UCL). If the charting statistic is plotted on or beyond the control limits, the process is said to be out-of-control (OOC).

Statistical process control (SPC) distinguishes two main types of charts, namely, memoryless (e.g., Shewhart-type charts) and memory-type (e.g., the cumulative sum (CUSUM) [1], exponentially weighted moving average (EWMA) [2] and homogeneously weighted moving average (HWMA) [3] as well as the CUSUM-, EWMA-, and HWM-related charts (see, e.g., Refs. [4–11])). Memoryless charts only focus on the most recent sample. In contrast, memory-type charts consider past and current samples, which are assigned weights summing up to one; see, e.g., Refs. [9,12]. Memory-type charts are known to be fast in detecting small and moderate shifts in the process parameters and slow in detecting large shifts. To improve the shift detection ability of the classical memory-type charts, many additional memory-type charts have been introduced in the literature, including the following:

(i) The extended EWMA charts (e.g., the double, triple, and quadruple EWMA (denoted as DEWMA, TEWMA, and QEWMA) charts), the classical extended EWMA (denoted as EEWMA) chart, and the modified EWMA (ModEWMA) chart; see, e.g., Refs. [10,13–15];

(ii) The CUSUM chart, dual CUSUM charts, and the generalization of the CUSUM chart; see, e.g., Refs. [16–19];
(iii) The generally weighted moving average (GWMA) chart by [11] and the double GWMA chart by [20] (see also [21]);
(iv) The extended HWMA charts (e.g., the double and triple HWMA (denoted as DHWMA and THWMA) charts) and the classical extended HWMA (denoted as EHWMA) chart; see, e.g., Refs. [22–24];
(v) The compound EWMA and HWMA charts (e.g., Shewhart–EWMA, Shewhart–CUSUM, mixed EWMA–CUSUM (MEC), mixed CUSUM–EWMA (MCE), mixed HWMA–CUSUM (MHC), and mixed CUSUM–HWMA (MCH) charts); see, e.g., Refs. [25–29].

A literature review is critical in understanding the research concepts on various topics as it gives an overview of the investigations conducted. It also guides researchers by providing possible research ideas that can be pursued concerning research gaps; see, e.g., Refs. [30,31]. This paper gives an overview of the HWMA-related charts and focuses on documenting and categorising all existing research articles discussing HWMA-related charts.

The HWMA chart was first introduced by [3] to improve the sensitivity of the EWMA chart in monitoring small shifts in the process parameter. Since then, there have been about 54 additional publications on HWMA-related charts. These research works were collected from when the first article was published (i.e., 2018). Only research articles and proceedings from accredited sources are considered, and other research documents such as books, theses, and dissertations are not considered. The research articles were collected from multiple scientific sources, publishers, and platforms such as John Wiley, Taylor and Francis, Springer Link, Emerald, Growing Science, Google Scholar, etc., by using keywords such as homogeneously weighted moving average, HWMA chart, statistical process control (SPC), statistical process monitoring (SPM), chart, etc., as well as references within the articles meeting the search criteria.

The rest of this paper is organised as follows: Section 2 discusses the weight functions of memory-type charts. Section 3 gives the basic properties of the HWMA-related charts for monitoring the process mean. In addition, Section 3 presents a detailed outline of how Section 4 categorizes the existing HWMA-related charts based on several criteria. Section 5 focuses on the controversies on the HWMA-related charts, and Section 6 gives some concluding remarks and future research ideas.

2. The Weight Function of the Most Popular Charts

The distribution of weights (or weight structure) amongst samples differs from one chart to the next. It is by this characteristic that the nature of a given chart can be identified. The shift detection ability of memory-type charts mainly depends on the weight structure of the charting statistics. Figure 1 displays the weight structure of the Shewhart, CUSUM, EWMA, and HWMA charts, which depicts the weights assigned to the first 20 observations (assuming samples of size one) used in calculating the charting statistic corresponding to the 20th sample (i.e., weight on the 20th charting statistic) when the smoothing parameter for the HWMA and EWMA charts is equal to 0.5 (i.e., $\lambda = 0.5$). Note that the 20th sample is designated as the *current sample* and the rest (i.e., samples 1 to 19) as *previous samples*. Figure 1 shows that for the EWMA chart, the weight assigned to previous samples decreases exponentially as the samples age; see also [32,33]. For instance, the current and 16th previous observations of the EWMA chart will be assigned weights of 0.5 and 0.03125, respectively. Thus, the older the sample, the smaller the weight. The weight assigned to the last 20 observations of the CUSUM chart from the current to the 20th previous observation is equal to 0.05, i.e., a uniform weight is assigned to the current and previous observations of the CUSUM chart; see also [34]. The HWMA chart assigns a weight of 0.5 to the current observation, and the rest of the observations are assigned a weight of $\frac{1-0.5}{19}$ (=0.026). Note, though, that the Shewhart chart focuses on the current sample with a weight of one, which is equivalent to the weight assigned to the EWMA chart with $\lambda = 1$. In other words, the weight used to compute the current charting statistic is equal to 1 for the t^{th} observation

and zero for all the previous ones. Figure 2 displays the weight structure of the HWMA chart for the first 20 observations for different smoothing parameters. This weight structure allows for the fast detection of small shifts in the process parameter(s). However, the HWMA chart detection ability for moderate and large shifts decreases.

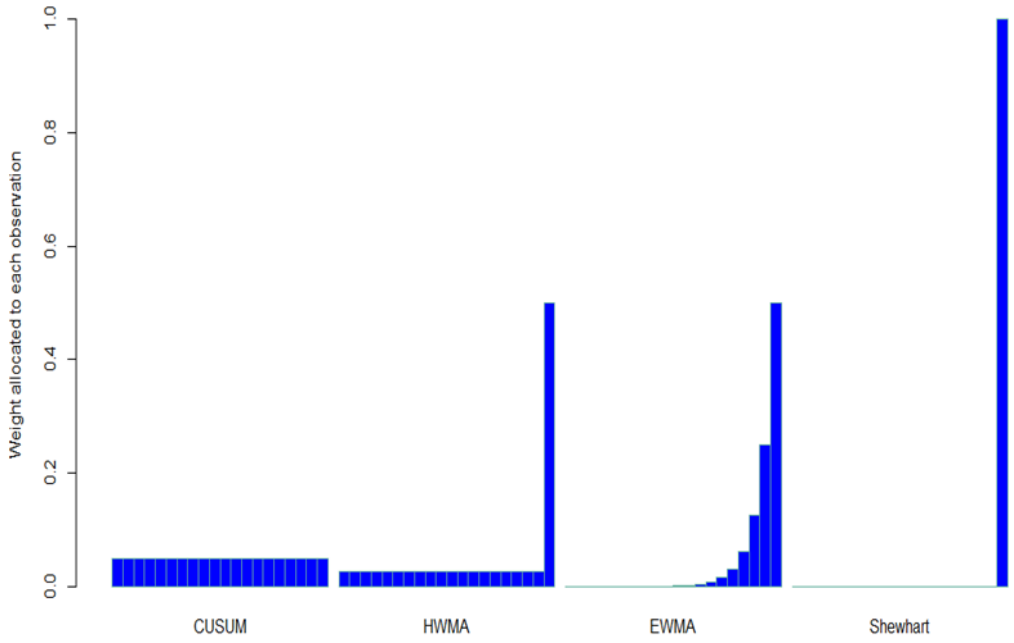

Figure 1. The numerical values of the weights for the Shewhart, EWMA (λ = 0.5), HWMA (λ = 0.5), and CUSUM charting statistics of the first 20 observations.

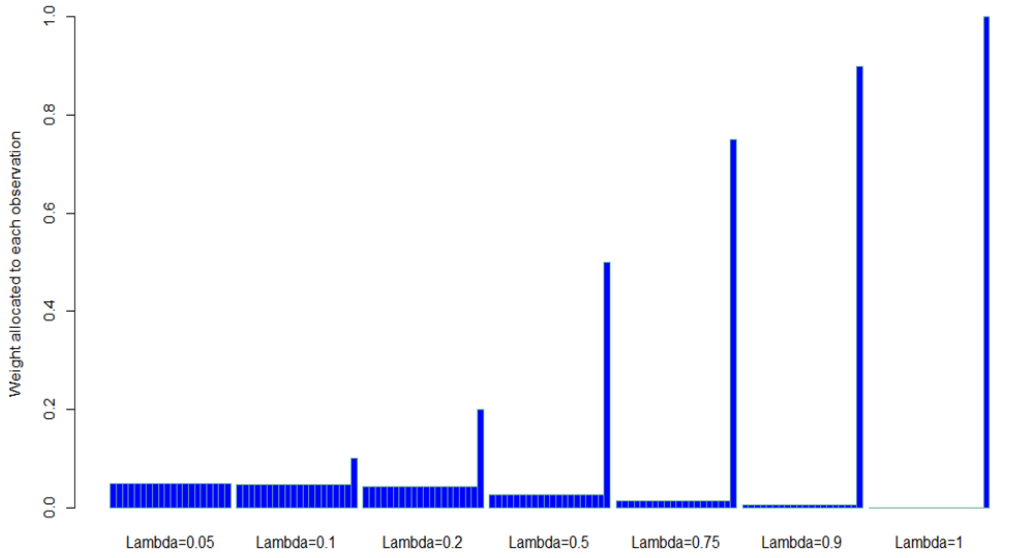

Figure 2. The numerical values of the weights of the HWMA charting statistics for the 20 first observations.

3. The Basic Properties of the HWMA and Enhanced HWMA Charts

3.1. Design of the HWMA and Enhanced HWMA Charts

This section illustrates the HWMA chart's design and its enhancements for the sample mean. To this end, assume that the quality characteristic of interest is a sequence of observations X_{tj} ($t = 1, 2, \ldots$ and $j = 1, 2, \ldots, n$), which are independent and identically distributed (i.i.d.) $N(\mu, \sigma)$ with known process parameters. When the process is in control

(IC), the IC mean and standard deviation are given by μ_0 and σ_0, respectively. Then, the charting statistic of the HWMA $\overline{X}$ chart (denoted as H_t) by [3] is defined by

$$H_t = \lambda \overline{X}_t + (1-\lambda)\, \overline{\overline{X}}_{t-1}, \tag{1}$$

with

$$\overline{\overline{X}}_{t-1} = \frac{1}{t-1}\sum_{v=1}^{t-1} \overline{X}_v,$$

where the smoothing parameter λ ranges from 0 to 1 and $\overline{\overline{X}}_{t-1}$ represents the mean of the previous $t-1$ sample means. Note that $\overline{\overline{X}}_0$, the initial value of $\overline{\overline{X}}_{t-1}$, is set to equal the IC mean μ_0. According to [3], Equation (1) can sometimes be written as

$$H_t = \lambda \overline{X}_t + \left(\left(\frac{1-\lambda}{t-1} \right) \overline{X}_{t-1} + \left(\frac{1-\lambda}{t-1} \right) \overline{X}_{t-2} + \cdots + \left(\frac{1-\lambda}{t-1} \right) \overline{X}_2 + \left(\frac{1-\lambda}{t-1} \right) \overline{X}_1 \right). \tag{2}$$

It can be deduced from Equation (2) that the HWMA $\overline{X}$ statistic assigns weight λ to the current sample, and a weight $(1-\lambda)$ is equally distributed to the previous $t-1$ samples. Furthermore, Abbas [3] indicated that the mean and variance of the charting statistic H_t are given by

$$E(H_t) = \mu_0 \text{and} Var(H_t) = \sigma^2_{H_t} = \begin{cases} \frac{\lambda^2 \sigma_0^2}{n}, & t = 1 \\ \frac{\lambda^2 \sigma_0^2}{n} + \frac{(1-\lambda)^2 \sigma_0^2}{n(t-1)}, & t > 1 \end{cases}, \tag{3}$$

respectively. Therefore, the time-varying lower and upper control limits, i.e., LCL_{H_t} and UCL_{H_t}, of the HWMA $\overline{X}$ chart are defined by

$$LCL_{H_t} = \begin{cases} \mu_0 - L_H \sqrt{\lambda^2 \frac{\sigma_0^2}{n}}, & t = 1 \\ \mu_0 - L_H \sqrt{\lambda^2 \frac{\sigma_0^2}{n} + (1-\lambda)^2 \frac{\sigma_0^2}{n(t-1)}}, & t > 1 \end{cases}$$

and

$$UCL_{H_t} = \begin{cases} \mu_0 + L_H \sqrt{\lambda^2 \frac{\sigma_0^2}{n}}, & t = 1 \\ \mu_0 + L_H \sqrt{\lambda^2 \frac{\sigma_0^2}{n} + (1-\lambda)^2 \frac{\sigma_0^2}{n(t-1)}}, & t > 1 \end{cases} \tag{4}$$

respectively, where the design parameter $L_H > 0$ determines the width of the control limits and it is selected such that the chart has an attained IC average run-length (ARL) approximately equal to some prespecified nominal IC ARL (ARL_0) such as 200, 370, or 500. For more details on how to search for the optimal design parameter L_H and compute the characteristics of the run-length distribution of the HWMA $\overline{X}$ chart, readers are referred to Appendix A. Thus, the HWMA $\overline{X}$ chart gives a signal when the charting statistic defined in Equation (1) plots on or outside the control limits defined in Equation (4); that is, if $H_t \geq UCL_{H_t}$ or $H_t \leq LCL_{H_t}$. In cases where the process is considered to have been running for a considerable time (i.e., $t \to \infty$), the term $\frac{(1-\lambda)^2 \sigma_0^2}{n(t-1)} \to 0$. Therefore, the control limits in Equation (4) reduce to the following asymptotic ones:

$$LCL = \mu_0 - L_H \frac{\lambda \sigma_0}{\sqrt{n}}$$

and

$$UCL = \mu_0 + L_H \frac{\lambda \sigma_0}{\sqrt{n}}. \tag{5}$$

The above expressions are summarised in Table 1 along with the charting statistics, design parameters, and control limits of the HHWMA, THWMA, HWMA–CUSUM, and CUSUM–HWMA $\overline{X}$ charts. Note that all starting values of the charting statistics of these

charts are typically set to be equal to the IC process mean (i.e., μ_0) except the one for the CUSUM-related chart, which is set to be equal to zero. When the smoothing parameters λ_1 and λ_2 of the HHWMA chart are equal, the HHWMA chart reduces to the DHWMA chart. For more details on the properties summarised in Table 1, readers are referred to [3,22,25,35–40].

Note that in Table 1, the underlying process parameters are assumed to be known (i.e., Case K), and the process monitoring can start immediately after computing the control limits that yield a desired attained IC ARL value; see, e.g., Refs. [13,26,38,41]. Typically, the process parameters are unknown (i.e., Case U). In this case, the process monitoring is implemented in two phases; the parameters are estimated in Phase I when the process is considered IC, and then, in Phase II, online monitoring is performed.

For more details on the design and implementation of HWMA-type charts, readers are referred to [3,25,42,43].

3.2. Performance Evaluation

The performance of a chart can be evaluated using the characteristics of the run-length distribution such as the ARL, the standard deviation of the run-length ($SDRL$), the median run-length (MRL), etc. The most popular performance measure is the ARL. This measure represents the average number of charting statistics to be plotted on a chart before the first OOC signal is observed. The run-length characteristics are often investigated using two different modes, namely, the zero- and steady-state modes; see, e.g., Ref. [44]. The zero- and steady-state run-length modes are used to investigate the short-term and the long-term run-length properties of a chart, respectively. The zero-state run-length is defined as the number of samples at which the chart first signals given that it begins in some specific initial state. However, the steady-state run-length is the number of samples at which the chart first signals given that the process begins and stays IC for a long period, and then at some random time, an OOC is observed; see, e.g., Refs. [44,45].

The zero- and steady-state run-lengths of the HWMA $\overline{X}$ chart denoted as L_Z and L_S are mathematically defined by (see, Refs. [45–47])

$$\begin{aligned} L_Z &= min\{t \geq 1 | H_t \leq LCL_{H_t} or\ H_t \geq UCL_{H_t}\} \\ \text{and} \\ L_S &= min\{t \geq \tau + 1 | H_t < LCL_{H_t} or\ H_t > UCL_{H_t}\},\ \tau = 1, 2, \ldots \end{aligned} \tag{6}$$

respectively; where τ is the change point applied in the change point model:

$$\mu = \begin{cases} \mu_0 = 0,\ if\ t < \tau \\ \mu_1 = \delta,\ if\ t \geq \tau' \end{cases} \tag{7}$$

where δ represents the change in the process mean.

For more details on how to compute the characteristics of the run-length distribution, readers are referred to Appendix A.

3.3. Outline of the Review

The structure of the review in Section 4 is outlined in Table 2. The "tick symbol" (i.e., "✓") indicates topics already treated, and the "cross symbol" (i.e., "×") indicates topics not yet published in the SPC literature.

For ease in identifying the different HWMA-type charts and their enhancements, in Table 3, the charts have been summarized with respect to the following characteristics:

(i) The process characteristic being monitored, i.e., the location (L), variability (V), both the location and variability (LV), or profile monitoring (P), e.g., for monitoring regression parameters and/or the regression error variance;
(ii) Whether the charts are parametric (Par) or nonparametric (NPar);
(iii) The design of the chart, i.e., economic (E), statistical (S), or economic statistical design (ESD);

(iv) Whether the underlying process parameters are known or unknown, i.e., Case K or Case U;
(v) The dimension of the process, i.e., univariate (Uni) or multivariate (Multi);
(vi) Whether the observations are i.i.d (IID) or autocorrelated (AC);
(vii) With measurement error (ME);
(viii) The mode, i.e., either zero-state (ZS) or steady-state (SS);
(ix) The type of data used in the illustrative examples, i.e., simulated (Sim) or real-life (Real) data;
(x) The number of citations (NC);
(xi) The performance metrics as discussed and used in the design;
(xii) The type of chart;
(xiii) The journal where the paper was published.

Note that Table 3 contains information about the HWMA-related articles that are the focus of this review paper. In this article, readers are also referred to other types of charts for general information. The list of acronyms used in this paper is given in Appendix B.

A summary of the journals and conference proceedings that published research on HWMA-type charts and their enhancements are provided in Table 4; this includes the type of journal, i.e., open access or hybrid, the ranking of the journal according to the journal citation reports (JCR) or proceedings, and the total number of publications. Table 4 shows that HWMA-type articles were published in 21 journals, and two were published as conference proceedings papers. Fifty percent of the journals in which these articles were published are open access, and the rest are hybrid journals. Eighteen out of fifty-five articles (i.e., 32.7%) were published in *Quality and Reliability Engineering International* (QREI), a quartile 2 journal. Note that according to the JCR ranking criteria, the top 25% of journals are classified in quartile 1, followed by the next 25% top journals in quartile 2, etc. From Table 4 and Figure 3, it can be noticed that 52% of the articles were published in quartile 2 journals and 35% were published in quartile 1 journals, followed by quartile 3 journals that published 13% of articles. No article was published in quartile 4; see Figure 3.

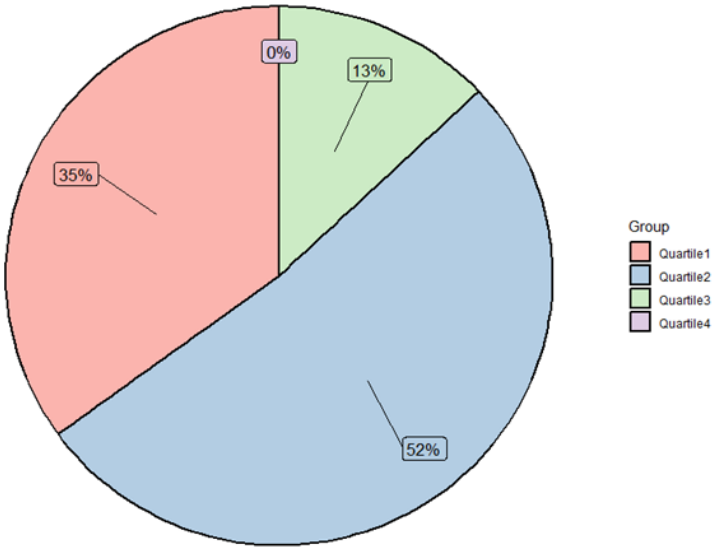

Figure 3. Amount (in percentage) of published HWMA-type articles according to the ranking category of journals.

Table 1. A summary of the charting statistics, design parameters, and control limits of the HWMA chart and its existing enhancements when the characteristic of interest is the process mean.

Chart	Charting Statistics	Design Parameters	Time-Varying Control Limits	Asymptotic Control Limits
HWMA	$H_t = \lambda \overline{X}_t + (1-\lambda)\,\overline{\overline{X}}_{t-1}$ where $\overline{\overline{X}}_0 = \mu_0$ and $\overline{\overline{X}}_{t-1} = \frac{1}{t-1}\sum_{v=1}^{t-1}\overline{X}_v$.	$L_H > 0$, $0 < \lambda \leq 1$	$LCL_{H_t} = \begin{cases} \mu_0 - L_H\sqrt{\lambda^2\frac{\sigma_0^2}{n}}, & t=1 \\ \mu_0 - L_H\sqrt{\lambda^2\frac{\sigma_0^2}{n} + (1-\lambda)^2\frac{\sigma_0^2}{n(t-1)}}, & t>1 \end{cases}$ and $UCL_{H_t} = \begin{cases} \mu_0 + L_H\sqrt{\lambda^2\frac{\sigma_0^2}{n}}, & t=1 \\ \mu_0 + L_H\sqrt{\lambda^2\frac{\sigma_0^2}{n} + (1-\lambda)^2\frac{\sigma_0^2}{n(t-1)}} & t>1 \end{cases}$.	$LCL_H = \mu_0 - L_H\sqrt{\lambda^2\frac{\sigma_0^2}{n}}$ and $UCL_H = \mu_0 + L_H\sqrt{\lambda^2\frac{\sigma_0^2}{n}}$.
HHWMA	$HH_t = \lambda_2 H_t + (1-\lambda_2)\,\overline{H}_{t-1}$ where $H_t = \lambda_1\overline{X}_t + (1-\lambda_1)\,\overline{\overline{X}}_{t-1}$, $\overline{H}_0 = \overline{\overline{X}}_0 = \mu_0$ and $\overline{H}_{t-1} = \frac{1}{t-1}\sum_{v=1}^{t-1} H_v$.	$L_{HH} > 0$, $0 < \lambda_1, \lambda_2 \leq 1$.	$LCL_{HH_t} = \mu_0 - L_{HH}\sqrt{Var(HH_t)}$ and $UCL_{HH_t} = \mu_0 + L_{HH}\sqrt{Var(HH_t)}$ where $Var(HH_t) = \begin{cases} \lambda_1^2\lambda_2^2\frac{\sigma_0^2}{n}, & \text{for } t=1 \\ \left[\lambda_1^2\lambda_2^2 + (\lambda_1+\lambda_2-2\lambda_1\lambda_2)^2\right]\frac{\sigma_0^2}{n}, & \text{for } t=2 \\ \left[\lambda_1^2\lambda_2^2 + term1 + term2\right]\frac{\sigma_0^2}{n}, & \text{for } t>2. \end{cases}$	$LCL_{HH} = \mu_0 - L_{HH}\sqrt{Var(HH_t)}$ and $UCL_{HH} = \mu_0 + L_{HH}\sqrt{Var(HH_t)}$ with $Var(HH_t) = \begin{cases} \lambda_1^2\lambda_2^2\frac{\sigma_0^2}{n}, & \text{for } t=1 \\ \left[\lambda_1^2\lambda_2^2 + (\lambda_1+\lambda_2-2\lambda_1\lambda_2)^2\right]\frac{\sigma_0^2}{n}, & \text{for } t=2 \\ \left[\lambda_1^2\lambda_2^2\right]\frac{\sigma_0^2}{n}, & \text{for } t>2. \end{cases}$
THWMA	$TH_t = \lambda DH_t + (1-\lambda)\,\overline{\overline{X}}_{t-1}$	$L_{TH} > 0$, $0 < \lambda \leq 1$	$LCL_{TH_t} = \mu_0 - L_{TH}\sqrt{Var(TH_t)}$ and $UCL_{TH_t} = \mu_0 + L_{TH}\sqrt{Var(TH_t)}$ where $Var(TH_t) = \begin{cases} \sqrt{\lambda^4\frac{\sigma_0^2}{n}}, & t=1 \\ \sqrt{\lambda^4\frac{\sigma_0^2}{n} + (1-\lambda^2)^2\frac{\sigma_0^2}{n(t-1)}}, & t>1 \end{cases}$	$LCL_{TH} = \mu_0 - L_{TH}\sqrt{\lambda^4\frac{\sigma_0^2}{n}}$ and $UCL_{TH} = \mu_0 + L_{TH}\sqrt{\lambda^4\frac{\sigma_0^2}{n}}$.
HWMA–CUSUM	$HC_t^+ = \max\left[0,\ (H_t - \mu_0 - k_H\sqrt{Var(H_t)}) + HC_{t-1}^+\right]$, and $HC_t^- = \max\left[0,\ \left(\mu_0 - H_t - k_H\sqrt{Var(H_t)}\right) + HC_{t-1}^-\right]$, with $HC_0^+ = HC_0^- = 0$	$k_H > 0$, $0 < \lambda \leq 1$, $h > 0$	$UCL_{HC_t} = h\sqrt{Var(H_t)}$	$UCL_{HC} = h\sqrt{\lambda^2\frac{\sigma_0^2}{n}}$

Table 1. *Cont.*

Chart	Charting Statistics	Design Parameters	Time-Varying Control Limits	Asymptotic Control Limits
CUSUM–HWMA	$CH_t^- = \lambda C_t^- + (1-\lambda)\,\overline{C}_{t-1}^-$ and $CH_t^+ = \lambda C_t^+ + (1-\lambda)\,\overline{C}_{t-1}^+$, where $C_t^- = \max\left[0,\ \left(\mu_0 - \overline{X}_t - k\frac{\sigma_0}{\sqrt{n}}\right) + C_{t-1}^-\right]$ and $C_t^+ = \max\left[0,\ (\overline{X}_t - \mu_0 - k\frac{\sigma_0}{\sqrt{n}}) + C_{t-1}^+\right]$ with $C_0^+ = C_0^- = 0$.	$L_{CH} > 0$, $0 < \lambda \leq 1$,	$LCL_{CH_t} = \begin{cases} \mu_{C_t} - L_{CH}\,(\lambda\sigma_{C_t}), & t = 1 \\ \mu_{C_t} - L_{CH}\,\sigma_{C_t}\sqrt{\lambda^2 + \frac{(1-\lambda)^2}{(t-1)}} & t > 1 \end{cases}$ and $UCL_{CH_t} = \begin{cases} \mu_{C_t} + L_{CH}\,(\lambda\sigma_{C_t}), & t = 1 \\ \mu_{C_t} + L_{CH}\,\sigma_{C_t}\sqrt{\lambda^2 + \frac{(1-\lambda)^2}{(t-1)}}, & t > 1 \end{cases}$ with $\mu_{C_t} = E(C_t^+) = E(C_t^-)$ and $\sigma_{C_t} = Var(C_t^+) = Var(C_t^-)$.	$LCL_{CH} = \mu_{C_t} - L_{CH}\,(\lambda\sigma_{C_t})$ and $UCL_{CH} = \mu_{C_t} + L_{CH}\,(\lambda\sigma_{C_t})$.

Note: $term1 = \frac{(\lambda_1+\lambda_2-2\lambda_1\lambda_2)^2}{(t-1)^2}$ and $term2 = \frac{1}{(t-1)^2}\sum_{u=1}^{t-2}\left(\lambda_1 + \lambda_2 - 2\lambda_1\lambda_2 + (1-\lambda_1)(1-\lambda_2)\sum_{k=u}^{t-2}\frac{1}{k}\right)^2$.

Table 2. Outline of the review in Section 4.

	Chart	Distribution	Section	Process Characteristic	Uni	Multi
Section 4.1	HWMA	Parametric	Section 4.1.1	Location	✓	✓
			Section 4.1.2	Variability	✓	×
			Section 4.1.3	Joint Location and Variability	✓	×
			Section 4.1.4	Profile	✓	✓
		Nonparametric	Section 4.1.5	Location	✓	✓
				Scale	×	×
			Section 4.1.6	Joint Location and Scale	✓	×
				Profile	×	×
Section 4.2	DHWMA and HHWMA	Parametric	Section 4.2.1	Location	✓	×
				Variability	×	×
			Section 4.2.2	Joint Location and Variability	✓	×
				Profile	×	×
		Nonparametric	Section 4.2.3	Location	✓	×
				Scale	×	×
				Joint Location and Scale	×	×
				Profile	×	×
Section 4.3	THWMA	Parametric	Section 4.3.1	Location	✓	×
			Section 4.3.2	Variability	✓	×
				Joint Location and Variability	×	×
				Profile	×	×
		Nonparametric	Section 4.3.3	Location	✓	×
				Scale	×	×
				Joint Location and Scale	×	×
				Profile	×	×
Section 4.4	HWMA-CUSUM & CUSUM-HWMA	Parametric	Section 4.4.1	Location	✓	×
				Variability	×	×
				Joint Location and Variability	×	×
				Profile	×	×
		Nonparametric		Location	×	×
				Scale	×	×
				Joint Location and Scale	×	×
				Profile	×	×

Note: Uni = univariate process; Multi = multivariate process.

Table 3. Classification of the articles discussing the HWMA-related charts.

Articles	L, V, LV, P	Par or NPar	E, SD, ESD	K	U	Dimension	IID	AC	ME	NC	Data	Mode	Performance Metrics	Type of HWMA Chart	Journal
Abbas [3]	L	Par	SD	✓	✓	Uni	✓			94	Real	ZS	*ARL*, *SDRL*	HWMA $\overline{X}$	CIE
Adegoke et al. [43]	L	Par	SD	✓	✓	Uni		✓		52	Sim	ZS	*ARL*, *SDRL*	HWMA $\overline{X}$ with AIB	IEEE Access
Adegoke et al. [48]	L	Par	SD	✓		Multi	✓			43	Sim, Real	ZS	*ARL*, *SDRL*	MHWMA T^2	IEEE Access
Nawaz and Han [49]	L	Par	SD	✓		Uni	✓			32	Real	ZS	*ARL*	HWMA $\overline{X}$ using RSS	QTQM
Abbas et al. [42]	L	Par	SD		✓	Multi	✓	✓		12	Real	ZS	*ARL*	MHWMA T^2	Mathematics
Abid et al. [25]	L	Par	SD	✓	✓	Uni	✓			35	Real	ZS	*ARL*, *SDRL*, *MRL*	DHWMA $\overline{X}$	QREI
Abid et al. [26]	L	Par	SD	✓		Uni	✓			25	Real	ZS	*ARL*, *SDRL*, *PRL*	HWMA–CUSUM $\overline{X}$	QREI
Abid et al. [50]	L	Par	SD	✓		Uni	✓			8	Real	ZS	*ARL*, *SDRL*, *PRL*	CUSUM–HWMA $\overline{X}$	QREI
Adeoti and Koleoso [51]	L	Par	SD	✓		Uni	✓			24	Sim	ZS	*ARL*, *SDRL*	HHWMA $\overline{X}$	QREI
Raza et al. [52]	L	NPar	SD	✓		Uni	✓			19	Real	ZS	*ARL*, *SDRL*, *MRL*, *EQL*	HWMA SN and SR	JTE
Riaz et al. [53]	L	NPar	SD	✓		Uni	✓			16	Real	ZS	*ARL*	DHWMA SN	QREI
Riaz et al. [41]	V	Par	SD	✓		Uni	✓			17	Real	ZS	*ARL*, *SDRL*, *MDRL*	HWMA S^2	Mathematics
Dawod et al. [54]	P	Par	SD		✓	Multi		✓		14	Real	ZS	*ARL*	HWMA profiles	CLS
Thanwane et al. [36]	L	Par	SD	✓		Uni	✓		✓	11	Real	ZS	*ARL*, *EARL*	HWMA $\overline{X}$	TIMC
Thanwane et al. [40]	L	Par	SD		✓	Uni	✓	✓	✓	7	Real	ZS	*ARL*, *SDRL*, *EARL*, *ESDRl*	HWMA $\overline{X}$	IEEE Access
Thanwane et al. [37]	L	Par	SD		✓	Uni	✓			6	Real	ZS	*ARL*, *SDRL*, *EARL*, *ESDRl*	HWMA $\overline{X}$ with FIR	QREI
Thanwane et al. [38]	L	Par	SD	✓		Uni		✓		2	Real	ZS	*ARL*, *SDRL*, *EARL*, *ESDRl*, *PCI*	HWMA $\overline{X}$	IJIEC
Thanwane et al. [39]	L	Par	SD		✓	Uni	✓		✓	13	Real	ZS	*ARL*, *EARL*	HWMA $\overline{X}$	JSCS
Alevizakos et al. [22]	L	Par	SD	✓		Uni	✓			13	Real, Sim	ZS	*ARL*, *SDRL*, *AEQL*, *PCI*, *RMI*	DHWMA & HHWMA $\overline{X}$	QREI
Alevizakos et al. [23]	L	NPar	SD	✓		Uni	✓			2	Real, Sim	ZS	*ARL*, *SDRL*, *MRL*, *AEQL*	DHWMA SN	QREI
Riaz et al. [24]	L	Par	SD		✓	Uni	✓			14	Real	ZS,SS	*ARL*, *SDRL*, *MDRL*	THWMA	Symmetry
Malela-Majika et al. [35]	L	Par	SD	✓		Multi	✓			3	-	ZS	*ARL*, *SDRL*, *MRL*	HHWMA	QREI

Table 3. *Cont.*

Articles	L, V, LV, P	Par or NPar	E, SD, ESD	K	U	Dimension	IID	AC	ME	NC	Data	Mode	Performance Metrics	Type of HWMA Chart	Journal
Adegoke et al. [55]	L	Par	SD		✓	Uni	✓			0	Real	ZS	*ARL*, *SDRL*	DSHWMA	QREI
Adegoke et al. [56]	L	Par	SD		✓	Multi	✓			2	Real	ZS,SS	*ARL*, *SDRL*	MHWMA	IEEE Access
Noor-ul-Amin and Noor [57]	L	Par	SD		✓	Uni	✓			1	Real	ZS	*ARL*, *SDRL*	HWMA $\overline{X}$ BTB	QREI
Adeoti et al. [58]	LV	Par	SD	✓		Uni	✓			10	Real, Sim	ZS	*ARL*, *SDRL*, *MRL*	HWMA (COM-Poisson)	JAS
Knoth et al. [44]	L	Par	SD	✓		Uni	✓			24	-	ZS,SS	*ARL* (*CED*)	HWMA with PM	QREI
Chan et al. [59]	LV	NPar	SD	✓		Uni	✓			16	Real	ZS	*ARL*, *EARL*, *PRL*	DEWMA–HWMA	CIE
Abbasi et al. [60]	V	Par	SD		✓	Uni	✓			3	Real		*ARL*, *SDRL*, *MRL*, *EQL*, *RARL*	HWMA dispersion	QREI
Abbasi et al. [61]	P	Par	SD	✓		Uni	✓			3	Real	ZS	*ARL*	HWMA profile	QREI
Rasheed et al. [62]	L	Par	SD	✓		Multi	✓			10	Real	ZS	*ARL*, *EQL*, *RARL*, *PCI*	MHWHC, MHCHW	MPE
Riaz et al. [63]	L	Par	SD	✓		Uni	✓			8	-	ZS,SS	*ARL*	HWMA	Processes
Aslam et al. [64]	L	Par	SD	✓		Uni	✓			1	Real	ZS	*ARL*, *SDRL*, *EQL*, *RARL*, *PCI*	HWMA TBE	QREI
Anwar et al. [65]	L	Par	SD	✓		Uni	✓			14	Real	ZS	*ARL*, *RARL*, *EQL*, *PCI*	DHWMA	QREI
Letshedi et al. [7]	L	NPar	SD		✓	Uni	✓			0	Real	ZS	*ARL*, *SDRL*, *EARL*, *ESDRL*	HWMA and HHWMA	PLoS one
Anwar et al. [66]	L	Par	SD	✓		Uni		✓		0	Real	ZS	*ARL*, *SDRL*, *MRL*, *EQL*, *RARL*, *PCI*	THWMA AIB	MPE
Al-Sayed et al. [67]	LV	Par	SD		✓	Uni		✓		0	Real	ZS	*ARL*, *RMI*	PR–HWMA, PR–DHWMA (ZIP)	IEEE ICIEEM
Rasheed et al. [68]	L	NPar	SD	✓		Uni	✓			8	Real	ZS	*ARL*, *SDRL*, *MRL*	DHWMA SR (RSS)	MPE
Chong et al. [69]	L	Par	SD	✓		Uni	✓			0	-	ZS	*ARL*, *SDRL*, *PRL*, *EARL*, *EMRL*	HWMA, DHWMA	IEEE ICIEEM
Iqbal et al. [70]	LV	Par	SD		✓	Uni		✓		13	Real	ZS	*ARL*, *SDRL*	HWMA and DHWMA DR, SDR	Symmetry
Zhang et al. [71]	L	NPar	SD	✓		Uni	✓			2	Real	ZS	*ARL*, *SDRL*, *MRL*	THWMA SR	MPE
Lone et al. [72]	L	Par	SD	✓		Uni	✓			3	Real	ZS	*ARL*, *SDRL*, *EQL*, *RARL*, *PCI*	THWMA TBE	AIMS Mathematics
Arslan et al. [73]	L	Par	SD	✓		Multi		✓		3	Real, Sim	ZS	*ARL*, *EQL*, *RMI*	TAHWMA	Symmetry

Table 3. *Cont.*

Articles	L, V, LV, P	Par or NPar	E, SD, ESD	K	U	Dimension	IID	AC	ME	NC	Data	Mode	Performance Metrics	Type of HWMA Chart	Journal
Yousefi et al. [74]	L	Par	SD	✓		Multi		✓	✓	4	Real	ZS	*ARL*, *SDRL*	MHWMA	JAMS
Almanjahie et al. [75]	L	NPar	SD	✓		Uni	✓			1	Real	ZS	*ARL*, *SDRL*, *MRL*, *EQL*, *RARL*, *PCI*	HWMA SR	CMES
Noor-ul-Amin and Arshad [76]	L	Par	SD	✓		Uni		✓		0	Real	ZS	*ARL*, *SDRL*	HWMA AIB	CS-SC
Anwer et al. [77]	L	Par	SD	✓		Uni		✓		1	Real	ZS	*ARL*, *PDARL*	HWMA–CUSUM AIB	JSCS
Knoth [78]	L	Par	SD	✓		Uni	✓			0	-	SS	*ARL*, *CED*	HWMA	QREI
Knoth et al. [47]	L	Par	SD	✓		Uni	✓			16	-	ZS,SS	*CED*	Memory-type	JQT
Khan et al. [79]	V	Par	SD	✓		Uni	✓			0	Real	ZS	*ARL*, *SDRL*, *EQL*, *RARL*, *PCI*	THWMAV	MPE
Pieters et al. [80]	L	Par	SD	✓		Multi	✓			1	Real	ZS,SS	*ARL*, *SDRL*	MEHWMA	QREI
Ghasemi et al. [81]	P	Par	SD	✓		Multi		✓		0	Sim	ZS	*ARL*	MHWMA	CS-SC
Zubair et al. [82]	L	Par	SD	✓		Uni		✓		0	Sim	ZS	*ARL*, *SDRL*, *MRL*	HWMA–CUSUM: AIB	PLoS one
Shafqat et al. [83]	L	NPar	SD	✓	✓	Uni		✓		0	Sim	ZS	*ARL*, *SDRL*, *MRL*	EWMA and HWMA SR: RS and AIB	Scientific Report
Sunthornwat et al. [84]	L	Par	SD	✓		Uni		✓		0	Real	ZS	*ARL*, *SDRL*, *MRL*, *EARL*, *EMRL*	Max HWMA	Symmetry

L = location; V = variability; LV = location and variability/scale; P = profile; Par = parametric; NPar = nonparametric; E = economic, SD = statistical design, ESD = economic statistical design; K = known; U = unknown; Uni = univariate process; Multi = multivariate process; IID = independent and identically distributed; AC = autocorrelated; ME = measurement error; AIB = auxiliary information based; SN = sign; SR = signed-rank; SDR = standardized residuals; RS = repetitive sampling; NC = number of citations; Real = real-life; Sim = simulation; CED = conditional expected delay; ZS = zero-state; SS = steady-state; *ARL* = average run-length; *SDRL* = standard deviation of the run-length; *MRL* = median run-length; *PRL* = percentile of the run-length; *PDARL* = percentage decrease *ARL*; *EARL* = expected *ARL*; *ESDRL* = expected *SDRL*; *EMRL* = expected *MRL*; *RARL* = relative average run-length; *EQL* = extra quadratic loss; *AEQL* = average *EQL*; *RMI* = relative mean index; *PCI* = performance comparison index; CMP = Conway–Maxwell–Poisson.

Table 4. Types and JCR rank of the journals/conference proceedings that published research on HWMA-type charts.

Journal/Conference Proceedings	Open Access/Hybrid	JCR Quartile	Number of Publications
Computers & Industrial Engineering (*CIE*)	Hybrid	1	2
Mathematics	Open access	1	2
Quality and Reliability Engineering International (*QREI*)	Hybrid	2	18
IEEE Access	Open Access	1	4
Journal of Applied Statistics (*JAS*)	Hybrid	2	1
IEEE International Conference on Industrial Engineering and Engineering Management (*IEEE ICIEEM*)	Open access	2	2
Computer Modeling in Engineering & Sciences (*CMES*)	Open access	3	1
Mathematical Problems in Engineering (*MPE*)	Open access	2	5
Journal of Statistical Computation and Simulation (*JSCS*)	Hybrid	2	2
Chemometrics and Laboratory Systems (*CLS*)	Hybrid	2	1
Symmetry	Open access	2	4
PLoS ONE	Open access	1	2
AIMS Mathematics	Open access	2	1
Quality Technology & Quantitative Management (*QTQM*)	Hybrid	1	1
Communications in Statistics-Simulation and Computation (*CS-SC*)	Hybrid	1	2
Journal Testing and Evaluation (*JTE*)	Open access	3	1
Processes	Open access	2	1
Scientific Reports	Open access	1	1
Transactions of the Institute of Measurement and Control (*TIMC*)	Hybrid	2	1
International Journal of Industrial Engineering Computations (*IJIEC*)	Hybrid	1	1
Journal of Advanced Manufacturing Systems (*JAMS*)	Hybrid	3	1
Journal of Quality Technology (*JQT*)	Hybrid	1	1

4. HWMA and Enhanced HWMA Charts

4.1. HWMA Charts

- **Parametric HWMA Charts**

4.1.1. Location

The HWMA chart for the process mean, i.e., the HWMA $\overline{X}$ chart, was introduced by Abbas (2018) to improve the detection ability of the EWMA $\overline{X}$ chart for monitoring small shifts. The charting statistic and control limits of the HWMA $\overline{X}$ chart are defined in Equations (1) and (4), respectively. In his paper, Abbas [3] compared the HWMA chart to the EWMA, CUSUM, and mixed EWMA–CUSUM (MEC) $\overline{X}$ charts in terms of their zero-state ARL ($ZSARL$) profiles. He reported that for small values of λ, the HWMA $\overline{X}$ chart outperforms the EWMA $\overline{X}$ chart for small shifts. However, for large λ values, the EWMA $\overline{X}$ chart performs better than the HWMA $\overline{X}$ chart for small to large shifts. Compared to the CUSUM $\overline{X}$ chart, the HWMA $\overline{X}$ chart performs better regardless of the magnitude of the shift. Compared to the MEC $\overline{X}$ chart, the HWMA $\overline{X}$ chart performs better for small λ values. However, for large λ values, the MEC $\overline{X}$ chart performs better.

Adegoke et al. [48] proposed an auxiliary-information-based (AIB) HWMA $\overline{X}$ chart for monitoring small shifts in the process mean with correlated auxiliary variables. They reported that the AIB HWMA $\overline{X}$ chart performs better than the classical HWMA $\overline{X}$ chart

and other competing charts (see [83]). Nawaz et al. (2020) designed the HWMA $\overline{X}$ chart using ranked set sampling (RSS) [49]. Thanwane et al. (2020) investigated the combined effect of autocorrelation and measurement error on the performance of the HWMA $\overline{X}$ chart [40].

4.1.2. Variability

Riaz et al. [41] proposed a one-sided HWMA chart for monitoring small shifts in the process dispersion. They discussed its performance in terms of the *ARL*, *SDRL*, and *MRL*. They found that the proposed HWMA chart performs better than the existing counterparts for small shifts.

Abbasi et al. [60] proposed an HWMA S chart to detect small shifts in the process standard deviation to monitor disturbances in the process dispersion. Their chart is used for the normal, heavy-tailed, symmetrical, and skewed underlying process distributions. Noor-ul-Amin and Arshad [76] proposed the HWMA S^2 chart for the fast detection of shifts in the variance. It was found that the proposed HWMA S^2 chart is sensitive to process shifts by using the auxiliary information with a high degree of correlation.

4.1.3. Joint Location and Variability

Adeoti et al. [58] proposed an HWMA chart based on the Conway–Maxwell–Poisson distribution, denoted as the CMP–HWMA chart, to monitor both the mean and dispersion when dealing with underspread and overspread count data. They investigated the performance of the CMP–HWMA chart for a range of shifts (including the overall performance) in terms of the *ARL*, *SDRL*, and *MRL* profiles along with the expected *ARL*, *SDRL*, and *MRL* metrics. They found that the CMP–HWMA chart performs better in many cases compared to other CMP memory-type charts. Al-Sayed et al. [67] proposed the HWMA chart based on the Pearson residuals (PR) of zero-inflated Poisson (ZIP) model, denoted as the PR–HWMA chart, to monitor small shifts in the location and variance simultaneously.

4.1.4. Profile

Dawod et al. [54] applied a Bayesian framework to construct HWMA-type charts for linear profiles to monitor the intercept, slope, and error variance for a linear regression applied in the pharmaceutical industry. Compared to the Shewhart, EWMA, CUSUM, and Hotelling's T^2 counterparts in terms of individual and overall performance metrics, the proposed HWMA charts outperform the competing charts, especially for small shifts in the regression parameters and error variance. A real-life example was used to illustrate the application of the proposed chart in shrinking the variations in the quality of a pharmaceutical product.

- **Nonparametric HWMA Charts**

4.1.5. Location

Raza et al. [52] proposed two nonparametric HWMA charts based on the sign (SN) and Wilcoxon signed-rank (SR) tests for monitoring deviations in the process location from the target value under skewed and symmetric distributions, respectively. These charts are denoted as the NPHWMA SN and NPHWMA SR charts. In their paper, Raza et al. [52] compared the proposed charts to the existing nonparametric EWMA and CUSUM SN and SR charts denoted as the NPEWMA and NPCUSUM SN and SR charts. They reported that the NPHWMA SN and NPHWMA SR perform better than their nonparametric counterparts. Recently, Shafqat et al. [83] proposed an AIB HWMA SR chart to improve the existing NPHWMA SR chart in monitoring small shifts in the process location parameter. Letshedi et al. [7] used a different nonparametric test, namely, the Wilcoxon rank-sum (WRS) test, to construct a nonparametric HWMA chart for monitoring very small shifts in the location parameter.

4.1.6. Joint Location and Scale

Chan et al. [59] proposed two nonparametric process monitoring schemes based on the double EWMA (DEWMA) and HWMA Lepage statistic for jointly monitoring a process's location and scale parameters. These charts' implementation and designs were based on the time-varying and asymptotic upper control limits. It was found that the HWMA Lepage (HL) chart with a time-varying control limit is better than the HL chart with the asymptotic control limit in reducing the rate of early false alarms. The DEWMA Lepage (DL) chart performs well in detecting small to moderate shifts in the process. The HL chart with the time-varying *UCL* performs better than the EWMA Lepage (EL) chart. In addition, the EL and DL charts are good with both time-varying and asymptotic control limits, but the HL chart works better only with the time-varying control limit.

To improve the HWMA-type chart, the literature in SPC proposes using the double or hybrid HWMA (i.e., DHWMA or HHWMA) chart. This is discussed in the next section.

4.2. DHWMA and HHWMA Charts

- **Parametric DHWMA and HHWMA Charts**

4.2.1. Location

Abid et al. [26] proposed the double HWMA (DHWMA) $\overline{X}$ chart to detect small disturbances in the process mean efficiently. Their results reveal that the DHWMA $\overline{X}$ chart is not IC robust, especially for large values of λ where, for instance, the attained IC *ARL* value can vary from 483.53 to 158.76 under the *Gamma* distribution and is much smaller under the *t* and *Logistic* distributions. Compared to the existing EWMA and HWMA $\overline{X}$ charts, they found that the DHWMA $\overline{X}$ chart is superior to the EWMA and HWMA $\overline{X}$ charts in many cases for various values of λ. Note that the DHWMA by Abid et al. [26] is just a reparameterisation of the HWMA chart where λ^2 is used instead of λ. Thus, Alevizakos et al. [22] extended the HWMA chart by imitating precisely the double EWMA (DEWMA) technique. Their chart is also denoted the DHWMA chart. A comparison study against the EWMA, DEWMA, HWMA, MEC, CUSUM, and the generally weighted moving average (GWMA) $\overline{X}$ charts showed that the DHWMA $\overline{X}$ chart is more effective in detecting small to moderate shifts. At the same time, it performs well against its competitors for large shifts. Alevizakos et al. [22] also studied the robustness of the DHWMA $\overline{X}$ chart under several non-normal distributions, and they found that the DHWMA $\overline{X}$ chart is IC robust for small values of λ. They also reported that the DHWMA $\overline{X}$ chart is more IC robust than the HWMA $\overline{X}$ chart regardless of the nature or type of the underlying process distribution. In addition, they showed that under the $t(\nu)$ and *Gamma*(α,1) distributions, the DHWMA $\overline{X}$ chart is more IC robust as ν and α increase. Adeoti and Koleoso [51] proposed the hybrid HWMA (HHWMA) $\overline{X}$ chart for monitoring the process mean. Malela-Majika et al. [35] corrected the variance used in the HHWMA $\overline{X}$ chart design proposed by [51]. For more details regarding the parametric DHWMA and HWMA charts for monitoring the location parameter, readers are referred to Alevizakos et al. [22,23,56,65].

4.2.2. Joint Location and Variability

Al-Sayed et al. [67] proposed the DHWMA chart based on the Pearson residuals (PR) of the ZIP model, denoted as the PR–DHWMA chart, to monitor small shifts in the location and variance simultaneously. They reported that the PR–HWMA chart performs relatively better than the PR–HWMA chart. Iqbal et al. [70] proposed the generalized linear model (GLM)-based HWMA and DHWMA charts based on the deviance residuals (DR) and standardized residuals (hereafter, SDR) of the Poisson regression model to monitor shifts in the location and variance simultaneously. These HWMA (DHWMA)-type charts are denoted the DR–HWMA (DR–DHWMA) and SDR–HWMA (SDR–DHWMA) charts. The authors concluded that the SDR–HWMA and SDR–DEWMA charts perform better than the DR–HWMA and DR–DHWMA charts. In addition, the SDR–DHWMA and DR–DHWMA charts outperform the SDR–HWMA and DR–HWMA charts, respectively.

- **Nonparametric DHWMA and HHWMA Charts**

4.2.3. Location

Riaz et al. [53] proposed the DHWMA SN chart, which is a reparameterisation of the HWMA SN chart. At the same time, Alevizakos et al. [23] mimicked the DEWMA SN chart and proposed the DHWMA SN chart for monitoring shifts in the location parameter. Compared to the HWMA, GWMA, double GWMA (DGWMA), triple exponentially weighted moving average (TWMA) SN charts, and classical DHWMA, it was found that the DHWMA SN chart performs better than the competing charts in many cases, especially for small shifts in the process parameter. Rasheed et al. [68] used the SR test to construct the DHWMA chart using RSS. Letshedi et al. [7] proposed the HWMA, DHWMA, and HHWMA charts based on the WRS W statistic, denoted as the W–HWMA, W–DHWMA, and W–HHWMA charts, for monitoring the location parameter. Their simulation results reveal the superiority and flexibility of the W–HHWMA chart over the W–HWMA, W–EWMA, and W–CUSUM charts.

4.3. THWMA Charts

- **Parametric THWMA Charts**

4.3.1. Location

Riaz et al. [24] extended the reparameterised DHWMA chart by introducing the triple HWMA (THWMA) chart. Anwar et al. [66] used auxiliary information to improve the THWMA chart proposed by [24]. Their results revealed that the AIB THWMA chart outperforms the classical THWMA chart, and both charts (i.e., THWMA and AIB THWMA) perform better than the DHWMA and AIB DHWMA, respectively. The THWMA chart for the time between events (TBE) was proposed by Lone et al. [72]. In their paper, Lone et al. [72] reported that the THWMA TBE outperforms the DHWMA TBE, HWMA TBE, EWMA TBE, and DEWMA TBE charts over a range of shifts.

Arslan et al. [73] proposed an HWMA chart using two supplementary variables; this chart is denoted as the TAHWMA chart. In their paper, they considered two supplementary variables that are correlated with the variable of interest in the form of a regression estimator, which is an efficient and unbiased estimator for the process location. The TAHWMA charting structure is studied and compared in terms of multicollinearity amidst the two additional variables. It was reported that the TAHWMA chart performs effectively when the two supplementary variables have no collinearity. A comparison between the TAHWMA and existing charts revealed the supremacy of the THWMA chart over its existing counterparts.

4.3.2. Variability

Khan et al. [79] proposed a one- and two-sided reparameterised THWMA chart for monitoring shifts in the process dispersion, and they reported the superiority of the THWMA chart over the DHWMA, HWMA, TEWMA, DEWMA, and EWMA charts in detecting shifts in the dispersion parameter.

- **Nonparametric THWMA and HHWMA Charts**

4.3.3. Location

Rasheed et al. [68] proposed a nonparametric THWMA SR chart using RSS, denoted as the NPTHWMA chart, to monitor shifts in the process location. The performance of the THWMA SR chart was investigated in terms of the *ARL*, *SDRL*, and *MRL* profiles. It was found that the THWMA SR chart is very sensitive to small shifts. The performance of this chart was compared to that of the NPTEWMA SR, TEWMA $\overline{X}$, and NPTEWMA SN charts and the NPTEWMA SR and NPDHWMA U charts using RSS. The comparison results revealed that the proposed NPTHWMA SR chart with RSS outperforms all competing charts considered in their paper, particularly for small to moderate shifts in the process location.

4.4. HWMA–CUSUM and CUSUM–HWMA Charts

- **Parametric HWMA Charts**

4.4.1. Location

The mixed HWMA–CUSUM (MHC) and mixed CUSUM–HWMA (MCH) $\overline{X}$ charts were proposed by Abid et al. [25] and Abid et al. [50], respectively, to enhance the shift detection ability of the CUSUM $\overline{X}$ and HWMA $\overline{X}$ charts in detecting small shifts in the process mean. The MHC and MCH $\overline{X}$ charts were compared to the CUSUM, EWMA, MEC, and HWMA $\overline{X}$ charts. In addition, the MHC $\overline{X}$ chart was compared to the MCE $\overline{X}$ chart. It was found that the MCH chart is quick in identifying any shifts in the process mean when compared to the CUSUM chart, while the MHC chart was found to be fast in detecting any shifts for all values of λ considered in the paper by Abid et al. [25]. The MHC chart performs better than the EWMA chart when $\lambda = 0.1$ for specific shifts. However, the MCH chart outperforms the EWMA chart in detecting small shifts when $\lambda = 0.1$. They also reported that as λ increases, the MCH exhibits a great sensitivity in detecting small to moderate shifts as compared to the EWMA and HWMA charts. It was also reported that the MCH performs relatively better than the MEC chart regardless of the magnitude of the shift in the process mean when $\lambda = 0.1$. When the shifts in the process mean are greater than 0.25 (i.e., $\delta > 0.25$), the MCH chart outperforms the MEC chart for large values of λ. The MHC chart is superior to the MEC and MCE charts when $\lambda = 0.1$ for small shifts. For large shifts, the MHC chart performs better than the MEC chart.

Anwer et al. [77] and Zubair et al. [82] proposed the AIB mixed HWMA–CUSUM (AIB–MHC) for monitoring the process mean. The results from these two papers showed that the AIB–MHC chart performs better than the AIB–HWMA chart for all choices of λ and correlation between the two variables (ρ) when $\delta < 0.75$. Compared to the AIB–MEC chart, the AIB–MHC chart presents a reasonably superior performance against the AIB–MEC chart for all choices of λ, ρ, and δ.

4.5. Multivariate Classical and Enhanced HWMA Charts

4.5.1. Location

Adegoke et al. [43] proposed a multivariate HWMA (MHWMA) chart for monitoring the process mean vector. The performance of this chart in terms of the *ARL* profile was evaluated and compared with the multivariate χ^2, MEWMA, and MCUSUM charts considering a variety of charting parameters. The comparison results revealed that the proposed MHWMA chart is superior to the competing charts, particularly in detecting small shifts in the process mean vector. Abbas et al. [42] investigated the effect of an estimated variance covariance matrix on the performance of the MHWMA T^2 chart and studied its performance in terms of the *ARL*, *SDRL*, *EQL*, and *RARL* for a wide range of the number of quality characteristics and varying sample sizes. Their performance analysis revealed that the MHWMA T^2 chart outperforms its multivariate counterparts under known and estimated process parameters. Later, Adegoke et al. [56] proposed one and two one-sided MHWMA charts for monitoring small shifts in the process mean vector, denoted as the OMHWMAI and OMHWMAII, respectively. The OMHWMAI chart is a one-sided chart for monitoring upward shifts by transforming the observation X_i into positive values. The OMHWMAII chart uses two one-sided MHWMA charts to monitor both upward and downward shifts in the process mean vector. The performances of these charts were evaluated in terms of their run-length properties for different shift sizes in the process mean vector. It was found that the OMHWMAII chart for monitoring upward shifts detects smaller shifts in the mean vector quicker than larger shifts. In contrast, the OMHWMAI chart, for monitoring upward shifts, detects larger shifts in the mean vector quicker than smaller shifts. In addition, the OMHWMAI and OMHWMA charts' sensitivities to non-normal distributions showed that they are remarkably robust to non-normality when a smaller value of λ is used. Thus, these charts can be designed to have an IC run-length performance that is very close to that of the charts based on normal distribution when a small value of λ is used.

Recently, Pieters et al. [80] proposed the multivariate extended HWMA (MEHWMA) chart by imitating the multivariate extended EWMA (MEEWMA) chart. This chart is designed to monitor small shifts in a multivariate process mean vector. To enable the identification of the variable that caused the OOC signal, a support vector machine was incorporated into the MEHWMA chart.

4.5.2. Profile

Ghasemi et al. [81] proposed three charts, namely, the MHWMA, MHWMA χ^2, and the combination of the MHWMA2 and mixed multivariate EWMA–CUSUM (denoted as MWHMA_2/MMECD) charts to monitor multivariate simple linear profiles efficiently. The performances of these three charts were evaluated in terms of their *ARL* profiles. Following a comprehensive comparison of the performance of these three charts, it was found that the MHWMA and MHWMA χ^2 charts perform better than MHWMA_2/MMECD chart for all shifts. Also, the MHWMA chart outperforms the MHWMA χ^2 chart in detecting small shifts, and the performance of these two charts is similar in detecting larger shifts.

For more details on the design of MHWMA-type charts, readers are referred to [42,56,74,80].

4.6. Other HWMA-Type Charts

Several other charts based on the HWMA statistics have been developed. Rasheed et al. [62] combined the HWMA chart's features with the existing mixed memory (MCE and MEC) charts to improve the shift detection ability of the mixed memory-type charts. The resulting charts are called the mixed HWMA homogeneously CUSUM (denoted as MHWHC) and mixed homogeneously CUSUM–HWMA (denoted as MHCHW) charts, respectively. The MHWHC and MHCHW charts' performances were compared to those of the classical CUSUM and EWMA, MEC, MCE, and HWMA charts. The comparison results revealed that the MHWHC and MHCHW charts are superior to their counterparts, specifically in detecting small and moderate shifts.

5. Controversies on the Practicality of the HWMA Chart

Several authors have criticized the weight structure of the HWMA chart. Knoth et al. [44] advised against the HWMA chart because it allocates equal weight to past samples, which greatly affects its performance, especially for small values of λ and at the start of any process monitoring regardless of the value of λ; see also Knoth [78]. They insisted that the zero-state performance of the HWMA chart that has been reported in the literature is deceptive since, in general, the steady-state kicks in from time $t > 1$, meaning that a memory-type chart practically runs in steady-state most of the time. After a thorough investigation of the steady-state performance of the HWMA chart using the conditional expected delay (CED) metric, they found that its performance was inferior to that of the other classical memory-type charts, i.e., the EWMA and CUSUM charts. In passing, they also advised against extending the HWMA and EWMA charts to more complex schemes for the same reasons; see also Knoth et al. [47]. Knoth et al. [47] reported that some of these charts, including compound charts such as the MEC, MCE, MCH, and MHC are found to be flawed and unnecessary.

Contrary to Knoth et al. [44] and Knoth [78], many authors encouraged the use of the HWMA chart because it has appealing zero-state properties and outperforms its counterparts in many cases in steady-state mode; see, e.g., Riaz et al. [63] and Anwar et al. [65]. Riaz et al. [63] reassessed the zero- and steady-state performances of the HWMA chart, following the criticism by [44], and reported that the weight structure of the HWMA chart can safeguard the detection ability and the run-length properties under various delays in process shifts. In addition, they showed that the HWMA chart is superior to the EWMA chart in many cases in the zero-state mode and can maintain its dominance if the process experiences a shift delay. However, in the steady-state mode, the performance of the HWMA chart depends on the suitable choice of design parameters.

5.1. Mathematical Background of the CED Metric

Kenett and Pollak [46] defined the CED as the delay from the first opportunity to detect a change and not from the time of the change itself. The CED, denoted as D_τ, is mathematically defined by

$$D_\tau = E_\tau(L - \tau + 1 | L \geq \tau),\ \tau = 1, 2, 3, \ldots, \tag{8}$$

where L represents the number of samples until an alarm is raised and τ is defined in Equation (6).

5.2. CED Performance Comparison

In this section, we present and discuss some results of the comparison analysis between the HWMA, EWMA, and CUSUM charts. These results are retrieved from the two important articles by Abbas [3] and Knoth et al. [44].

Table 5 compares the performances of the HWMA ($\lambda = 0.05$), HWMA ($\lambda = 0.1$), EWMA ($\lambda = 0.05$), EWMA ($\lambda = 0.1$), CUSUM ($k = 0.125$), and CUSUM ($k = 0.225$) charts in terms of the $ZSARL$ profile, where k is the reference value of the CUSUM chart. From Table 5, it can be seen that the HWMA chart outperforms the EWMA chart for very small shifts, i.e., $0 < \delta \leq 0.25$. However, for moderate to large shifts, the EWMA chart performs better than the HWMA chart. In addition, Table 5 reveals the superiority of the HWMA chart over the CUSUM chart regardless of the magnitude of the shift.

Table 5. Zero-state performance comparison of the HWMA, EWMA, and CUSUM charts.

Shift	HWMA (λ= 0.05)	EWMA (λ = 0.05)	CUSUM (k = 0.125)	HWMA (λ = 0.1)	EWMA (λ = 0.1)	CUSUM (k = 0.225)
0.25	73.01	77.76	83.39	81.48	103.32	91.16
0.5	24.92	23.71	34.65	28.61	28.81	31.19
0.75	12.78	11.87	21.68	14.85	13.61	18.01
1	8.04	7.31	15.78	9.35	8.21	12.63
1.5	4.4	3.77	10.26	4.98	4.17	7.94
2	2.98	2.43	7.64	3.32	2.66	5.83
2.5	2.2	1.77	6.12	2.45	1.92	4.65
3	1.67	1.41	5.13	1.87	1.51	3.89
5	1.01	1.01	3.19	1.03	1.02	2.41

Figure 4 compares the performances of the HWMA and EWMA charts in terms of the CED profile when $\lambda = 0.1$. Note that when τ = 1, the CED profile is equivalent to the conditional $ZSARL$ profile denoted by D_1, and when $\tau > 1$, it is equivalent to the conditional steady-state ARL ($SSARL$) profile denoted by D_τ with $\tau \neq 1$. From Figure 4, it can be seen that when $\delta = 0.25$, in zero-state mode, the HWMA chart performs better than the EWMA chart. However, in steady-state mode, the HWMA outperforms the EWMA for $\tau < 53$. When $0 < \delta \leq 1$, the EWMA chart performs better than the HWMA chart regardless of the value of τ. Note that for small shifts, the D_τ profile of the HWMA chart is an increasing function of τ, while the D_τ profile of the EWMA chart converges towards fixed values for different shifts. This clearly shows that the steady-state performance of the HWMA chart is worse than that of the EWMA chart (see Figure 4a). For large shifts, the D_τ profile of the EWMA chart is smaller than that of the HWMA chart when $0 \leq \delta < 3$. When $\delta = 3$ and 5, the EWMA chart performs better than the HWMA chart for $\tau \leq 220$ and $\tau \leq 50$, respectively. As τ increases, when δ = 3 and 5, the HWMA chart outperforms the EWMA chart for $\tau > 220$ and $\tau > 50$, respectively (see Figure 4b).

From the above discussion, it can be seen that the EWMA chart performs better than the HWMA chart in many cases. However, it must not be ignored that the HWMA chart performs better in some of the cases.

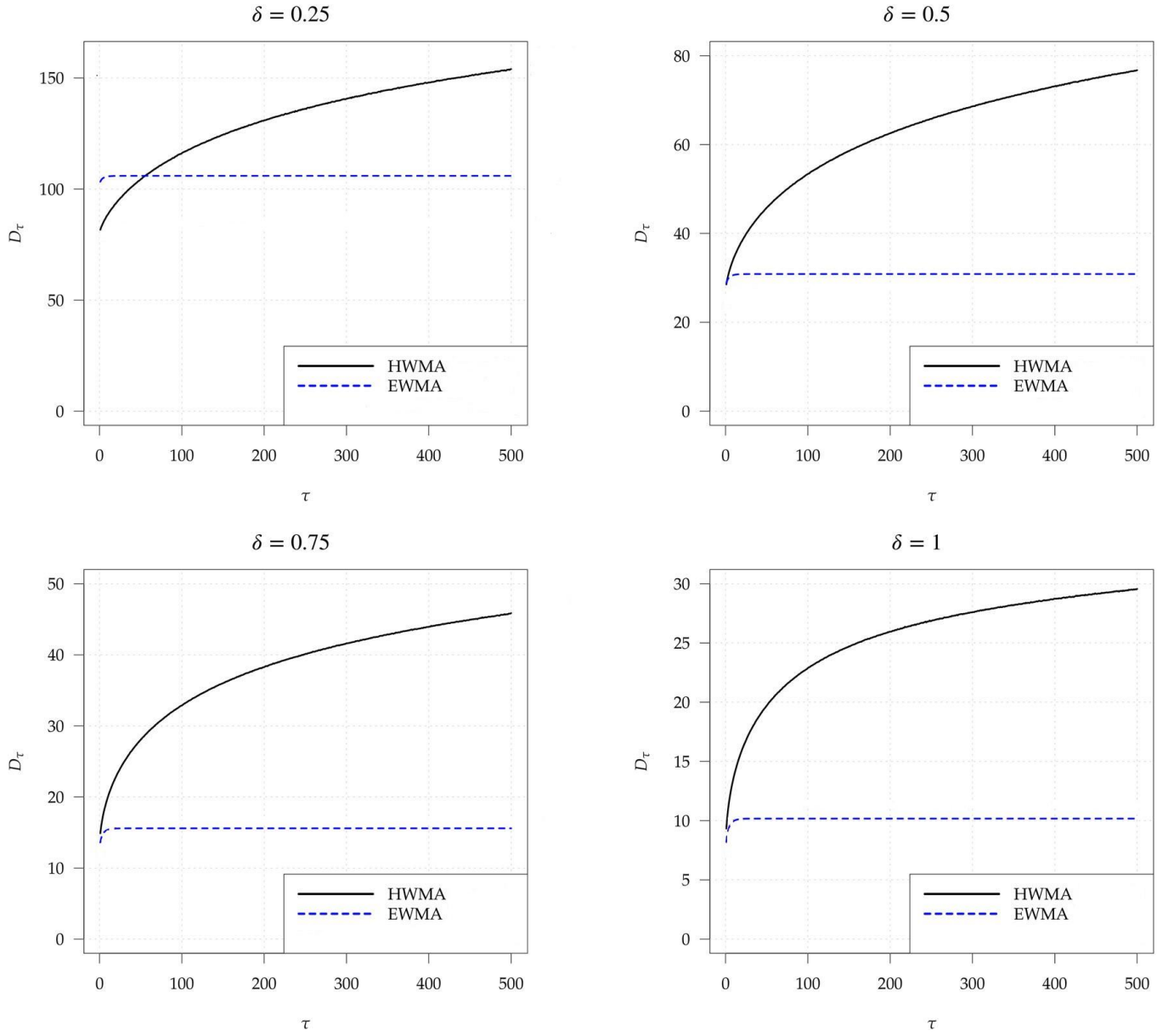

(**a**) Zero- and steady-state performances for small shifts.

Figure 4. *Cont.*

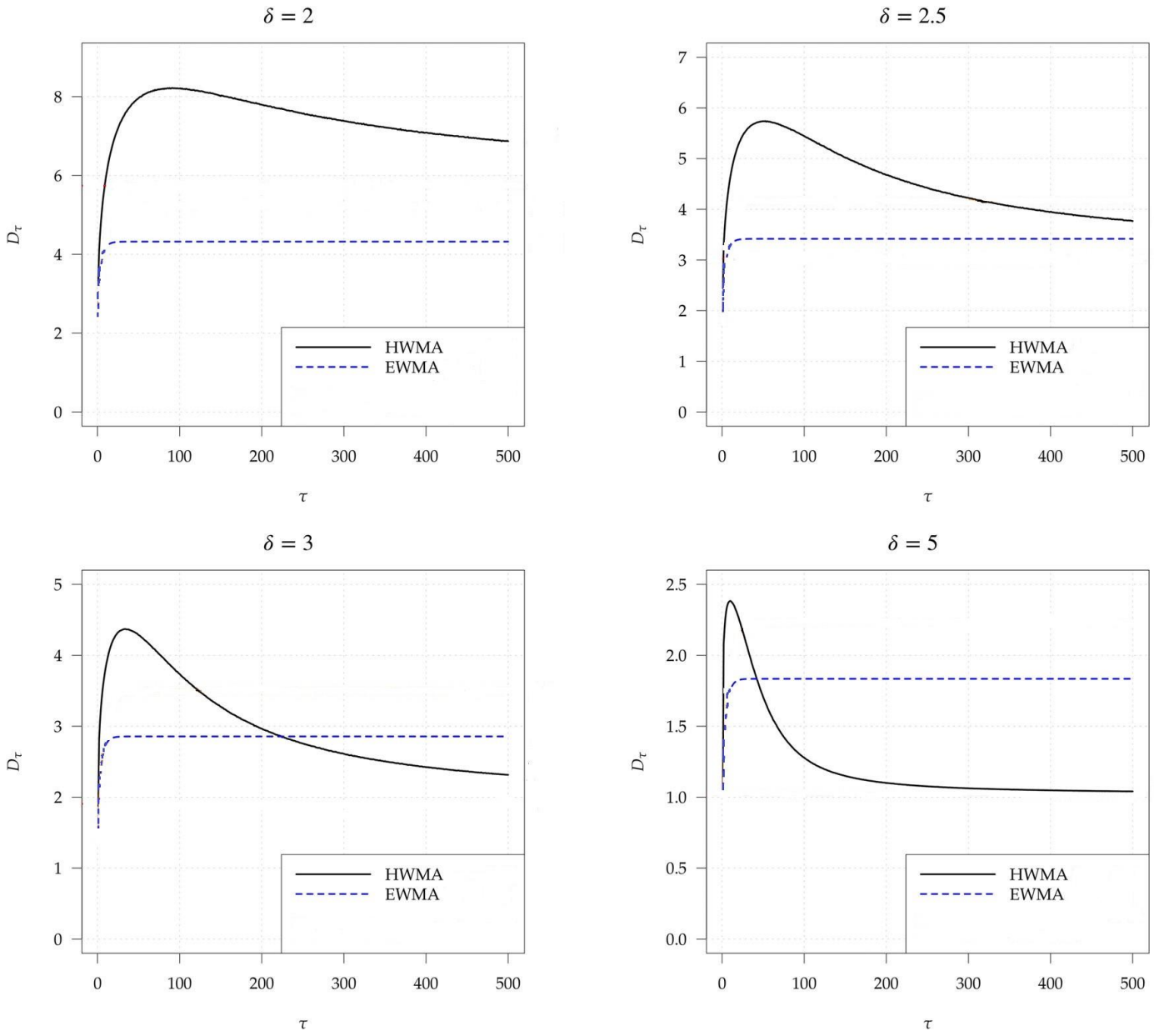

(**b**) Zero- and steady-state performances for moderate and large shifts.

Figure 4. Zero- and steady-state performance comparison of the HWMA and EWMA charts.

6. Conclusions, Recommendation, Future Research Work, and New Directions

In this paper, we reviewed the HWMA chart and its associated enhancements. The HWMA chart is a memory-type chart that assigns a specific weight to the most recent sample and the rest is distributed equally between previous samples. A thorough review of the HWMA and HWMA-related charts, i.e., DHWMA, THWMA, HWMA–CUSUM, CUSUM–HWMA, etc., was documented, and based on the observations from the published literature, it was seen that these charts have excellent detection ability for small shifts when compared to the corresponding CUSUM- and EWMA-type charts (including their enhancements).

The HWMA and memory-type charts received criticism; see, e.g., Refs. [44,47]. Knoth et al. [44] advised against the use of the HWMA chart in practice because of its incapacity to detect changes that occur after the start-up period of the process due to its incoherent weight structure. We acknowledge that this constructive criticism fosters a healthy debate and improves the research quality. This review aimed to consolidate the recent developments

and provide future research ideas based on the gaps identified, not conclude the debate. Thus, below, we provide a summary of topics that have not yet been addressed:

(i) Most quality characteristics are dependent on one or more independent variables. In this case, profile monitoring can be used. However, only three articles on profile monitoring are available in the literature; hence, researchers interested in profile monitoring can construct charts using different regression models and investigate their performance.

(ii) Parametric and nonparametric HWMA charts with unknown process parameters under the assumption of i.i.d. and correlated observations are scarce. More research and thorough investigations regarding the performances of these types of charts are required.

(iii) No publications in nonparametric statistical monitoring for compound HWMA-type charts exist; hence, more research needs to be conducted to address this gap.

(iv) To enhance the literature on HWMA charts, researchers are encouraged to conduct additional research focusing on parametric and nonparametric HWMA charts with unknown process parameters, particularly under the assumptions of i.i.d. and correlated observations. A comprehensive exploration study about the zero- and steady-state performances of these types of charts would significantly contribute to the existing body of knowledge.

(v) The literature has various parametric and nonparametric synthetic charts using structured and unstructured sampling techniques (e.g., RSS, VSS, variable sample size and interval (VSSI), etc.). However, there is no work on synthetic HWMA and HWMA-related charts. Interested researchers can investigate this topic using different sampling structures.

(vi) Measurement errors (or imperfect measurements) are widespread in SPC applications and have been shown to harm the performance of any chart. Only the performance of the standard HWMA chart has been investigated under imperfect measurements. Thus, researchers are encouraged to consider this when designing extended and compound HWMA-type charts.

(vii) There are few parametric and nonparametric HWMA-type charts for joint monitoring of the process mean and variability (or process location and scale). Researchers are encouraged to use different test statistics to construct new HWMA-type charts.

(viii) Evaluating the characteristics of the run-length of charts using exact formulae, is critical; hence, more research on these topics is needed to simplify the evaluation of the run-length properties of the HWMA and HWMA-related charts.

(ix) The application of the HWMA-type charts in practice in various disciplines such as healthcare services and engineering is recommended.

(x) Only a few attribute HWMA charts have been proposed in the literature. More investigations on attribute HWMA charts as well as high-yield processes are needed.

(xi) There is no study on the economic and economic–statistical designs of the HWMA-type charts. Therefore, researchers are encouraged to investigate these topics under the assumption of i.i.d, serial dependency, perfect and imperfect measurements, and the combined effect of autocorrelation and measurement errors.

(xii) Only three publications on multivariate HWMA charts are available in the literature. Given the relevance of multivariate charts in applications, there is a lot of research on HWMA-type charts that can be conducted based on parametric and nonparametric settings for monitoring the location, variability, profile, joint location, and variability of multivariate processes.

(xiii) Researchers are advised to consider the weight structure when designing memory-type charts. The best weight structure will likely be the one that allocates small weights to previous samples.

(xiv) In practice, most applications are characterized by several quality characteristics that depend on one or several variables; in such cases, charts for multivariate profiles are more appropriate. Tables 2 and 3 show that there is a significant gap in the literature

concerning the HWMA-related charts for monitoring multivariate processes. Thus, researchers are encouraged to design efficient classical multivariate charts as well as linear and nonlinear profile HWMA charts considering the effect of multicollinearity and dependence structure.

(xv) Recent advances in information technology (IT) have enabled researchers to collect, store, and easily access large volumes of data at a modest cost. Researchers are encouraged to look at the design of multivariate HWMA-related charts for monitoring high-dimensional profile data.

(xvi) Researchers are encouraged to continue the collaborative dialogue between critics and proponents of the HWMA chart, fostering a comprehensive understanding of its strengths and limitations. This inclusive approach will contribute to addressing research gaps and improve the overall quality of research in the field of SPC.

Author Contributions: Authors equally contributed to the paper. All authors have read and agreed to the published version of the manuscript.

Funding: This research received no external funding.

Acknowledgments: The second author thanks the South African National Research Foundation (NRF) for their support under the grant (RA210125583099) and the Research Development Programme at the University of Pretoria, Department of Research and Innovation (DRI).

Conflicts of Interest: The authors have no conflicts of interest.

Appendix A. Simulation Algorithm

This appendix explains how to compute the IC and OOC zero- and steady-state characteristics of the run-length distribution for the HWMA $\overline{X}$ chart in the case of a normal distribution using s simulation runs. This is carried out in two stages:

Stage 1—First, we search for the value of the design parameter L_H that gives an attained IC ARL value as close as possible to the specified ARL_0 value. If such a value exists, L_H is called the optimal design parameter.

Stage 2—The optimal design parameter is used to compute OOC ARL values.

Note that in Steps 5 and 10, other characteristics of the run-length distribution, such as the $SDRL$ and the percentiles of the run-length (PRL), can also be computed. Moreover, the above simulation algorithm can be adjusted to accommodate distributions and statistics (e.g., the standard deviation or variance in case monitoring the spread is of importance) by modifying the distribution from which the random sample is generated and the charting statistic in Steps 3 and 8.

Step	Zero-State Mode	Steady-State Mode
	Stage 1—Search for the optimal value of L_H:	
1	Specify the ARL_0 value, the sample size (n), the number of simulations (s), the smoothing parameter (λ), and the parameters of the distribution.	Specify the value of $\tau > 1$, the ARL_0 value, the sample size (n), the number of simulations (s), the smoothing parameter (λ), and the parameters of the distribution.
2	(a) Set L_H to some value, compute the control limits, and proceed to Step 3. (b) Whenever necessary, increase (or decrease) the L_H value, then recompute the control limits to attain an IC ARL value that approaches ARL_0.	
3	Generate a random sample from the $N(0,1)$ distribution. Compute the charting statistic and compare it to the control limits found in Step 2. When the charting statistic plots between the control limits, generate the next sample, calculate its charting statistic, and compare it with the control limits. Continue this process until a charting statistic plots on or outside the control limits. This means that the process has gone OOC. Record the number of samples generated until an OOC signal occurs. This number represents one simulated value of the IC run-length distribution.	Generate a random sample from the $N(0,1)$ distribution. Compute the charting statistic and compare it to the control limits found in Step 2. When the charting statistic plots between the control limits, generate the next sample, calculate its charting statistic, and compare it with the control limits. Continue this process until a charting statistic plots on or outside the control limits provided $t \geq \tau$. This means that the process has gone OOC. Record the number of samples, L, generated until an OOC signal occurs. Then, calculate $L - \tau + 1$. This value represents one simulated value of the IC run-length distribution.
4	Repeat Step 3 a total of s times to find the $(s \times 1)$ IC run-length vector of simulated observations ($\boldsymbol{RL}_0$)	
5	Once the $\boldsymbol{RL}_0$ vector is obtained, we compute the average, which we call the attained IC ARL value, i.e., $$\text{IC } ARL = \frac{1}{s}\sum_{i=1}^{s} RL_{0_i}. \quad \text{(A1)}$$ If the attained IC ARL value is equal or much closer to the ARL_0, go to Step 6. Otherwise, if the attained IC ARL is considerably smaller (greater) than the ARL_0 value, then go back to Step 2 (b) to update the control limits to be wider (narrower) by increasing (decreasing) the L_H value. Note that the variance of the point estimator in Equation (A1) decreases as the number of simulations increases.	
6	The latest value of L_H used in Step 5 is considered as the optimal design parameter. Record the optimal L_H value and the corresponding control limits. Thus, the search for the optimal L_H is completed.	
	Stage 2—Computation of the characteristics of the OOC run-length:	
7	Specify a nonzero value of δ, i.e., $\delta \neq 0$, which represents the size of the shift in the process mean.	

Step	Zero-State Mode	Steady-State Mode
8	Generate a random sample from the $N(\delta,1)$ distribution. Then, compute its charting statistic and compare it to the control limits found in Step 6. When the charting statistic plots between the control limit, generate the next sample, calculate its charting statistic, and compare it with the control limits. Continue this process until a charting statistic plots on or outside the control limits. When this happens, record the number of samples generated until an OOC signal occurs. This number represents one value of the OOC run-length distribution.	Generate a random sample from the $N(\delta,1)$ distribution. Then, compute its charting statistic and compare it to the control limits found in Step 6. When the charting statistic plots between the control limits then generate the next sample, calculate its charting statistic, and compare it with the control limits. Continue this process until a charting statistic plots on or outside the control limits provided $t \geq \tau$. When this happens, record the number of samples, L, generated until an OOC signal occurs. Then, calculate $L - \tau + 1$. This number represents one simulated value of the OOC run-length distribution.
9	Repeat Step 8 a total of s times to find the $(s \times 1)$ OOC run-length vector of simulated observations ($\boldsymbol{RL}_1$).	
10	One the $\boldsymbol{RL}_1$ vector is obtained, compute the attained OOC ARL (ARL_1) value as $ARL_1 = \frac{1}{s}\sum_{i=1}^{s} RL_{1_i}$. (A2) This value represents the ARL_1 value for a shift of δ standard deviation.	

Appendix B. List of Acronyms

Acronyms	Description
AEQL	Average extra quadratic loss
AIB	Auxiliary information based
ARL	Average run-length
CED	Conditional expected delay
CIE	*Computers & Industrial Engineering*
CLS	*Chemometrics and Laboratory Systems*
CMES	*Computer Modeling in Engineering & Sciences*
CMP	Conway–Maxwell–Poisson
CS-SC	*Communications in Statistics-Simulation and Computation*
CUSUM	Cumulative sum
DEWMA	Double exponentially weighted moving average
DGWMA	Double generally weighted moving average
DHWMA	Double homogeneously weighted moving average
DR	Deviance residuals
EARL	Expected average run-length
EEWMA	Extended exponentially weighted moving average
EMRL	Expected median run-length
EQL	Extra quadratic loss
ESD	Economic statistical design
ESDRL	Expected standard deviation of the run-length
EWMA	Exponentially weighted moving average
GLM	Generalized linear model
GWMA	Generally weighted moving average
HHWMA	Hybrid homogeneously weighted moving average
HWMA	Homogeneously weighted moving average
IC	In-control
IEEE ICIEEM	*IEEE International Conference on Industrial Engineering and Engineering Management*
i.i.d.	Independent and identically distributed
IJIEC	*International Journal of Industrial Engineering Computations*
JAMS	*Journal of Advanced Manufacturing Systems*
JAS	*Journal of Applied Statistics*
JCR	Journal citation reports
JQT	*Journal of Quality Technology*
JSCS	*Journal of Statistical Computation and Simulation*
JTE	*Journal Testing and Evaluation*
MCE	Mixed CUSUM–EWMA
MCH	Mixed CUSUM–HWMA

MCUSUM	Multivariate cumulative sum
ME	Measurement error
MEC	Mixed EWMA–CUSUM
MEEWMA	Multivariate extended exponentially weighted moving average
MEHWMA	Multivariate extended homogeneously weighted moving average
MHC	Mixed HWMA–CUSUM
MHWMA	Multivariate homogeneously weighted moving average
ModEWMA	Modified exponentially weighted moving average
MPE	*Mathematical Problems in Engineering*
MRL	Median run-length
NC	Number of citations
OOC	Out-of-control
PCI	Performance comparison index
PDARL	Percentage decrease average run-length
PR	Pearson residual
PRL	Percentile of the run-length
QEWMA	Quadruple exponentially weighted moving average
QREI	*Quality and Reliability Engineering International*
QTQM	*Quality Technology & Quantitative Management*
RARL	Relative average run-length
RMI	Relative mean index
RS	Repetitive sampling
RSS	Ranked set sampling
SD	Statistical design
SDRL	Standard deviation of the run-length
SPC	Statistical process control
SPM	Statistical process monitoring
SR	Signed-rank
SS	Steady-state
SSARL	Steady-state average run-length
TBE	Time between events
TEWMA	Triple exponentially weighted moving average
THWMA	Triple homogeneously weighted moving average
TIMC	*Transactions of the Institute of Measurement and Control*
WRS	Wilcoxon rank-sum
ZIP	Zero-inflated Poisson
ZS	Zero-state
ZSARL	Zero-state average run-length

References

1. Page, E. Continuous inspection schemes. *Biometrika* **1954**, *41*, 100–115. [CrossRef]
2. Roberts, S.W. Control chart tests based on geometric moving averages. *Technometrics* **1959**, *1*, 239–250. [CrossRef]

3. Abbas, N. Homogeneously weighted moving average control chart with an application in substrate manufacturing process. *Comput. Ind. Eng.* **2018**, *120*, 460–470. [CrossRef]
4. Haq, A.; Munir, T.; Khoo, M.B.C. Dual multivariate CUSUM mean charts. *Comput. Ind. Eng.* **2019**, *137*, 106028. [CrossRef]
5. Haq, A.; Munir, T.; Shah, B.A. Dual multivariate CUSUM charts with auxiliary information for process mean. *Qual. Reliab. Eng. Int.* **2020**, *36*, 861–875. [CrossRef]
6. Lee, M.H.; Khoo, M.B.C. Optimal statistical designs of a multivariate CUSUM chart based on ARL and MRL. *Int. J. Reliab. Qual. Saf. Eng.* **2006**, *13*, 479–497. [CrossRef]
7. Letshedi, T.I.; Malela-Majika, J.-C.; Shongwe, S.C. New extended distribution-free homogenously weighted monitoring schemes for monitoring abrupt shifts in the location parameter. *PLoS ONE* **2022**, *17*, e0261217. [CrossRef] [PubMed]
8. Lowry, C.A.; Woodall, W.H.; Champ, C.W.; Rigdon, S.E. A multivariate exponentially weighted moving average control chart. *Technometrics* **1992**, *34*, 46–53. [CrossRef]
9. Montgomery, D.C. *Introduction to Statistical Quality Control*, 8th ed.; John Wiley & Sons: Hoboken, NJ, USA, 2020; ISBN 978-1-119-72309-7.
10. Shamma, S.E.; Shamma, A.K. Development and evaluation of control charts using double exponentially weighted moving averages. *Int. J. Qual. Reliab. Manag.* **1992**, *9*, 18–26. [CrossRef]
11. Sheu, S.-H.; Lin, T.-C. The generally weighted moving average control chart for detecting small shifts in the process mean. *Qual. Eng.* **2003**, *16*, 209–231. [CrossRef]
12. Srivastava, M.S.; Wu, Y. Evaluation of optimum weights and average run lengths in EWMA control schemes. *Commun. Stat. Theory Methods* **1997**, *26*, 1253–1267. [CrossRef]
13. Alevizakos, V.; Chatterjee, K.; Koukouvinos, C. The triple exponentially weighted moving average control chart. *Qual. Technol. Quant. Manag.* **2021**, *18*, 326–354. [CrossRef]
14. Alevizakos, V.; Chatterjee, K.; Koukouvinos, C. The quadruple exponentially weighted moving average control chart. *Qual. Technol. Quant. Manag.* **2022**, *19*, 50–73. [CrossRef]
15. Alkahtani, S.; Schaffer, J.A. Double multivariate exponentially weighted moving average (dEWMA) control chart for a process location monitoring. *Commun. Stat.-Simul. Comput.* **2012**, *41*, 238–252. [CrossRef]
16. Crosier, R.B. Multivariate generalizations of cumulative sum quality-control schemes. *Technometrics* **1988**, *30*, 291–303. [CrossRef]
17. Haq, A.; Ali, Q. A maximum dual CUSUM chart for joint monitoring of process mean and variance. *Qual. Technol. Quant. Manag.* **2023**. [CrossRef]
18. Haq, A.; Syed, E.A. New CUSUM and dual CUSUM mean charts. *Qual. Reliab. Eng. Int.* **2021**, *37*, 1355–1372. [CrossRef]
19. Wang, T.; Huang, S. An adaptive multivariate CUSUM control chart for signaling a range of location shifts. *Commun. Stat. Theory Methods* **2016**, *45*, 4673–4691. [CrossRef]
20. Sheu, S.H.; Hsieh, Y.T. The extended GWMA control chart. *J. Appl. Stat.* **2009**, *36*, 135–147. [CrossRef]
21. Phengsalae, Y.; Areepong, Y.; Sukparungsee, S. An Approximation of ARL for Poisson GWMA using Markov Chain Approach. *Thail. Stat.* **2015**, *13*, 111–124.
22. Alevizakos, V.; Chatterjee, K.; Koukouvinos, C. The extended homogeneously weighted moving average control chart. *Qual. Reliab. Eng. Int.* **2021**, *37*, 2134–2155. [CrossRef]
23. Alevizakos, V.; Chatterjee, K.; Koukouvinos, C. The extended nonparametric homogeneously weighted moving average sign control chart. *Qual. Reliab. Eng. Int.* **2021**, *37*, 3395–3416. [CrossRef]
24. Riaz, M.; Abbas, Z.; Nazir, H.Z.; Abid, M. On the development of triple homogeneously weighted moving average control chart. *Symmetry* **2021**, *13*, 360. [CrossRef]
25. Abid, M.; Mei, S.; Nazir, H.Z.; Riaz, M.; Hussain, S. A mixed HWMA-CUSUM mean chart with an application to manufacturing process. *Qual. Reliab. Eng. Int.* **2020**, *37*, 618–631. [CrossRef]
26. Abid, M.; Shabbir, A.; Nazir, H.Z.; Sherwani, R.A.K.; Riaz, M. A double homogeneously weighted moving average control chart for monitoring of the process mean. *Qual. Reliab. Eng. Int.* **2020**, *36*, 1513–1527. [CrossRef]
27. Ajadi, J.O.; Riaz, M. Mixed multivariate EWMA-CUSUM control charts for an improved process monitoring. *Commun. Stat. Theory Methods* **2017**, *46*, 6980–6993. [CrossRef]
28. Osei-Aning, R.; Abbasi, S.A.; Riaz, M. Mixed EWMA-CUSUM and mixed CUSUM-EWMA for monitoring first order autoregressive processes. *Qual. Technol. Quant. Manag.* **2017**, *14*, 429–453. [CrossRef]
29. Ottenstreuer, S.; Weiß, C.H.; Knoth, S. A combined Shewhart-CUSUM chart with switching limit. *Qual. Eng.* **2019**, *31*, 255–268. [CrossRef]
30. Snyder, H. Literature Review as a Research Methodology: An Overview and Guidelines. *J. Bus. Res.* **2019**, *104*, 333–339. [CrossRef]
31. Suman, G.; Prajapati, D.R. Control chart applications in healthcare: A literature review. *Int. J. Metrol. Qual. Eng.* **2018**, *9*, 5. [CrossRef]
32. Císar, P.; Cisar, S.M. Optimization Methods of EWMA Statistics. *Acta Polytech. Hung.* **2012**, *8*, 73–87.
33. Neuburger, J.; Walker, K.; Sherlaw-Johnson, C.; van der Meulen, J.; Cromwell, D.A. Comparison of control charts for monitoring clinical performance using binary data. *BMJ Qual. Saf.* **2017**, *26*, 919–928. [CrossRef]
34. Vera do Carmo, C.; Lopes, L.F.D.; Souza, A.M. Comparative study of the performance of the CUSUM and EWMA control charts. *Comput. Ind. Eng.* **2004**, *46*, 707–724.

35. Malela-Majika, J.-C.; Shongwe, S.C.; Adeoti, O.A. A hybrid homogeneously weighted moving average control chart for process monitoring: Discussion. *Qual. Reliab. Eng. Int.* **2021**, *37*, 3314–3322. [CrossRef]
36. Thanwane, M.; Abbasi, S.A.; Malela-Majika, J.-C.; Aslam, M.; Shongwe, S.C. The use of fast initial response features on the homogeneously weighted moving average chart with estimated parameters under the effect of measurement errors. *Qual. Reliab. Eng. Int.* **2021**, *37*, 2568–2586. [CrossRef]
37. Thanwane, M.; Malela-Majika, J.-C.; Castagliola, P.; Shongwe, S.C. The effect of measurement errors on the performance of the homogeneously weighted moving average $\overline{X}$ monitoring scheme with estimated parameters. *J. Stat. Comput. Simul.* **2021**, *91*, 1306–1330. [CrossRef]
38. Thanwane, M.; Malela-Majika, J.-C.; Castagliola, P.; Shongwe, S.C. The effect of measurement errors on the performance of the homogeneously weighted moving average $\overline{X}$ monitoring scheme. *Trans. Inst. Meas. Control* **2021**, *43*, 728–745. [CrossRef]
39. Thanwane, M.; Sandile, S.C.; Aslam, M.; Malela-Majika, J.-C.; Albassam, M. A homogenously weighted moving average scheme for observations under the effect of serial dependence and measurement inaccuracy. *Int. J. Ind. Eng. Comput.* **2021**, *12*, 401–414. [CrossRef]
40. Thanwane, M.; Shongwe, S.C.; Malela-Majika, J.-C.; Aslam, M. Parameter estimation effect of the homogeneously weighted moving average chart to monitor the mean of autocorrelated observations with measurement errors. *IEEE Access* **2020**, *8*, 221352–221366. [CrossRef]
41. Riaz, M.; Abbasi, S.A.; Abid, M.; Hamzat, A.K. A new HWMA dispersion control chart with an application to wind farm data. *Mathematics* **2020**, *8*, 2136. [CrossRef]
42. Abbas, N.; Riaz, M.; Ahmad, S.; Abid, M.; Zaman, B. On the efficient monitoring of multivariate processes with unknown parameters. *Mathematics* **2020**, *8*, 823. [CrossRef]
43. Adegoke, N.A.; Abbasi, S.A.; Smith, A.N.H.; Anderson, M.J.; Pawley, M.D.M. A multivariate homogeneously weighted moving average control chart. *IEEE Access* **2019**, *7*, 9586–9597. [CrossRef]
44. Knoth, S.; Tercero-Gómez, V.G.; Khakifirooz, M.; Woodall, W.H. The impracticality of homogeneously weighted moving average and progressive mean control chart approaches. *Qual. Reliab. Eng. Int.* **2021**, *37*, 3779–3794. [CrossRef]
45. Knoth, S. Steady-state average run length(s): Methodology, formulas, and numerics. *Seq. Anal.* **2012**, *40*, 405–426. [CrossRef]
46. Kenett, R.; Pollak, M. On assessing the performance of sequential procedures for detecting a change. *Qual. Reliab. Eng. Int.* **2012**, *28*, 500–507. [CrossRef]
47. Knoth, S.; Saleh, N.A.; Mahmoud, M.A.; Woodall, W.H.; Tercero-Gómez, V.G. A critique of a variety of "memory-based" process monitoring methods. *J. Qual. Technol.* **2023**, *55*, 18–42. [CrossRef]
48. Adegoke, N.A.; Smith, A.N.H.; Anderson, M.J.; Sanusi, R.A.; Pawley, M.D.M. Efficient homogeneously weighted moving average chart for monitoring process mean using an auxiliary variable. *IEEE Access* **2019**, *7*, 94021–94032. [CrossRef]
49. Nawaz, T.; Han, D. Monitoring the process location by using new ranked set sampling-based memory control charts. *Qual. Technol. Quant. Manag.* **2020**, *17*, 255–284. [CrossRef]
50. Abid, M.; Mei, S.; Nazir, H.Z.; Riaz, M.; Hussain, S.; Abbas, Z. A mixed cumulative sum homogeneously weighted moving average control chart for monitoring process mean. *Qual. Reliab. Eng. Int.* **2021**, *37*, 1758–1771. [CrossRef]
51. Adeoti, O.A.; Koleoso, S.O. A hybrid homogeneously weighted moving average control chart for process monitoring. *Qual. Reliab. Eng. Int.* **2020**, *36*, 2170–2186. [CrossRef]
52. Raza, M.; Nawaz, T.; Han, D. On designing distribution-free homogeneously weighted moving average control charts. *J. Test. Eval.* **2020**, *48*, 3154–3171. [CrossRef]
53. Riaz, M.; Abid, M.; Shabbir, A.; Nazir, H.Z.; Abbas, Z.; Abbasi, S.A. A non-parametric double homogeneously weighted moving average control chart under sign statistic. *Qual. Reliab. Eng. Int.* **2021**, *37*, 1544–1560. [CrossRef]
54. Dawod, A.; Adegoke, N.A.; Abbasi, S.A. Efficient linear profile schemes for monitoring bivariate correlated processes with applications in the pharmaceutical industry. *Chemom. Lab. Syst.* **2020**, *206*, 104137. [CrossRef]
55. Adegoke, N.A.; Ganiyu, K.O.; Abbasi, S.A. Directionally sensitive homogeneously weighted moving average control charts. *Qual. Reliab. Eng. Int.* **2021**, *37*, 3465–3492. [CrossRef]
56. Adegoke, N.A.; Riaz, M.; Ganiyu, K.O.; Abbasi, S.A. One-sided and two one-sided multivariate homogeneously weighted moving charts for monitoring process mean. *IEEE Access* **2021**, *9*, 80388–80404. [CrossRef]
57. Noor-ul-Amin, M.; Noor, S. Homogeneously weighted moving average control chart based on Bayesian theory. *Qual. Reliab. Eng. Int.* **2021**, *37*, 3617–3637. [CrossRef]
58. Adeoti, O.A.; Malela-Majika, J.-C.; Shongwe, S.C.; Aslam, M. A homogeneously weighted moving average control chart for Conway–Maxwell Poisson distribution. *J. Appl. Stat.* **2022**, *49*, 3090–3119. [CrossRef] [PubMed]
59. Chan, K.M.; Mukherjee, A.; Chong, Z.L.; Lee, H.C. Distribution-free double exponentially and homogeneously weighted moving average lepage schemes with an application in monitoring exit rate. *Comput. Ind. Eng.* **2021**, *161*, 107370. [CrossRef]
60. Abbasi, S.A.; Nassar, S.H.; Aldosari, M.M.; Adeoti, O.A. Efficient homogeneously weighted dispersion control charts with an application to distillation process. *Qual. Reliab. Eng. Int.* **2021**, *37*, 3221–3241. [CrossRef]
61. Abbasi, S.A.; Abbas, T.; Adegoke, N.A. Improved simple linear profiling method with application to chemical gas sensors. *Qual. Reliab. Eng. Int.* **2021**, *37*, 3179–3191. [CrossRef]
62. Rasheed, Z.; Zhang, H.; Anwar, S.M.; Zaman, B. Homogeneously mixed memory charts with application in the substrate production process. *Math. Probl. Eng.* **2021**, 2582210. [CrossRef]

63. Riaz, M.; Ahmad, S.; Mahmood, T.; Abbas, N. On reassessment of the HWMA chart for process monitoring. *Processes* **2022**, *10*, 1129. [CrossRef]
64. Aslam, M.; Khan, M.; Anwar, S.M.; Zaman, B. A homogeneously weighted moving average control chart for monitoring time between events. *Qual. Reliab. Eng. Int.* **2022**, *38*, 1013–1044. [CrossRef]
65. Anwar, S.M.; Aslam, M.; Zaman, B.; Riaz, M. An enhanced double homogeneously weighted moving average control chart to monitor process location with application in automobile field. *Qual. Reliab. Eng. Int.* **2022**, *38*, 174–194. [CrossRef]
66. Anwar, S.M.; Komal, S.; Cheema, A.N.; Abiodun, N.L.; Rasheed, Z.; Khan, M. Efficient control charting scheme for the process location with application in automobile Industry. *Math. Probl. Eng.* **2022**, 2938878. [CrossRef]
67. Al-Sayed, A.M.; Mahmood, T.; Saleh, H.H. Residual Based Control Charts for Zero-inflated Poisson Processes. In Proceedings of the 2022 IEEE International Conference on Industrial Engineering and Engineering Management (IEEM), Kuala Lumpur, Malaysia, 7–10 December 2022; pp. 482–486. [CrossRef]
68. Rasheed, Z.; Khan, M.; Abiodun, N.L.; Anwar, S.M.; Khalaf, G.; Abbasi, S.A. Improved nonparametric control chart based on ranked set sampling with application of chemical data modelling. *Math. Probl. Eng.* **2022**, *2022*, 7350204. [CrossRef]
69. Chong, Z.L.; Chan, K.M.; Wang, J.; Malela-Majika, J.-C.; Shongwe, S.C. Overall performance comparison of homogeneously weighted moving average and double homogeneously weighted moving average schemes. In Proceedings of the 2021 IEEE International Conference on Industrial Engineering and Engineering Management (IEEM), Singapore, 13–16 December 2021; pp. 1225–1229.
70. Iqbal, A.; Mahmood, T.; Ali, Z.; Riaz, M. On enhanced GLM-Based monitoring: An application to additive manufacturing process. *Symmetry* **2022**, *14*, 122. [CrossRef]
71. Zhang, H.; Rasheed, Z.; Khan, M.; Namangale, J.J.; Anwar, S.M.; Hamid, A. A distribution-free THWMA control chart under ranked set sampling. *Math. Probl. Eng.* **2022**, *2022*, 3823013. [CrossRef]
72. Lone, S.A.; Rasheed, Z.; Anwar, S.; Khan, M.; Anwar, S.M.; Shahab, S. Enhanced fault detection models with real-life applications. *AIMS Math.* **2023**, *8*, 19595–19636. [CrossRef]
73. Arslan, M.; Anwar, S.; Gunaime, N.M.; Shahab, S.; Lone, S.A.; Rasheed, Z. An improved charting scheme to monitor the process mean using two supplementary variables. *Symmetry* **2023**, *15*, 482. [CrossRef]
74. Yousefi, S.; Maleki, M.R.; Salmasnia, A.; Anbohi, M.K. Performance of multivariate homogeneously weighted moving average chart for monitoring the process mean in the presence of measurement errors. *J. Adv. Manuf. Syst.* **2023**, *22*, 27–40. [CrossRef]
75. Almanjahie, I.M.; Rasheed, Z.; Khan, M.; Anwar, S.M.; Cheema, A.N. Ranked-set sampling based distribution free control chart with application in CSTR process. *Comput. Model. Eng. Sci.* **2023**, *135*, 2091–2118. [CrossRef]
76. Noor-ul-Amin, M.; Arshad, A. Homogeneously weighted moving average-variance control chart using auxiliary information. *Commun. Stat. Simul. Comput.* **2023**, *52*, 4891–4908. [CrossRef]
77. Anwer, F.; Sanaullah, A.; Ahmad, A.; Asghar, A. An improved mixed-homogeneously weighted moving average-CUSUM control chart for efficient monitoring of a process mean. *J. Stat. Comput. Simul.* **2023**, *93*, 1644–1666. [CrossRef]
78. Knoth, S. Another objection to the homogeneously weighted moving average control chart. *Qual. Reliab. Eng. Int.* **2023**, *39*, 353–362. [CrossRef]
79. Khan, M.; Rasheed, Z.; Anwar, S.M.; Namangale, J.J. Triple homogeneously weighted moving average charts for monitoring Process Dispersion. *Math. Probl. Eng.* **2023**, 6996280. [CrossRef]
80. Pieters, L.; Malela-Majika, J.-C.; Human, S.W.; Castagliola, P. A new multivariate extended homogeneously weighted moving average monitoring scheme incorporated with a support vector machine. *Qual. Reliab. Eng. Int.* **2023**, *39*, 2454–2475. [CrossRef]
81. Ghasemi, Z.; Hamadani, A.H.; Yazdi, A.A. New methods for phase II monitoring of multivariate simple linear profiles. *Commun. Stat. Simul. Comput.* **2023**, 1–25. [CrossRef]
82. Zubair, F.; Sherwani, R.A.K.; Abid, M. Enhanced performance of mixed HWMA-CUSUM charts using auxiliary information. *PLoS ONE* **2023**, *18*, e0290727. [CrossRef]
83. Shafqat, A.; Zhensheng, H.; Aslam, M. Efficient signed-rank based EWMA and HWMA repetitive control charts for monitoring process mean with and without auxiliary information. *Sci. Rep.* **2013**, *13*, 16459. [CrossRef] [PubMed]
84. Sunthornwat, R.; Sukparungsee, S.; Areepong, Y. Analytical explicit formulas of average run length of homogenously weighted moving average control chart based on a MAX process. *Symmetry* **2023**, *15*, 2112. [CrossRef]